

# Modulation of Tropical Convection-circulation Interaction by Aerosol Indirect Effects in a Global Convection-permitting Model

Chun-Yian Su<sup>1</sup>, Chien-Ming Wu<sup>2</sup>, Wei-Ting Chen<sup>2</sup>, and John Peters<sup>3</sup>

<sup>1</sup>Pennsylvania State University

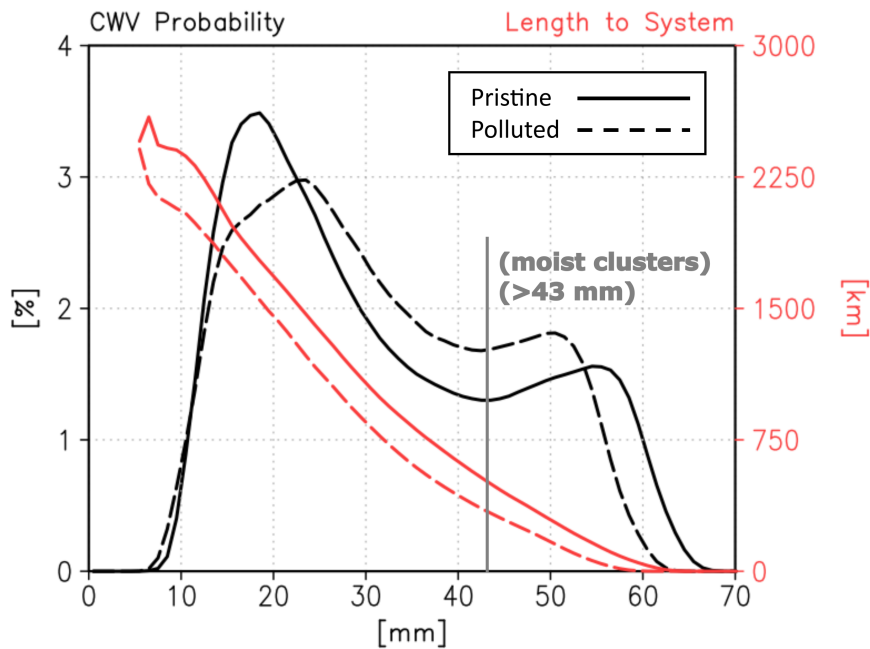
<sup>2</sup>National Taiwan University

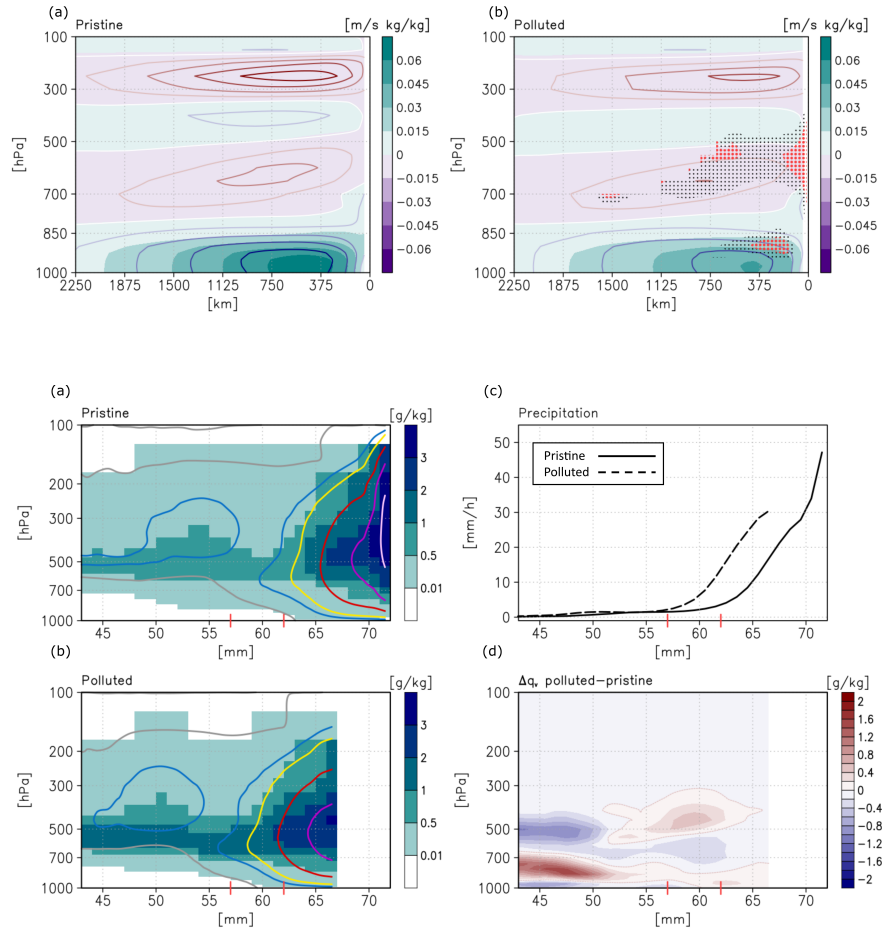
<sup>3</sup>Penn State

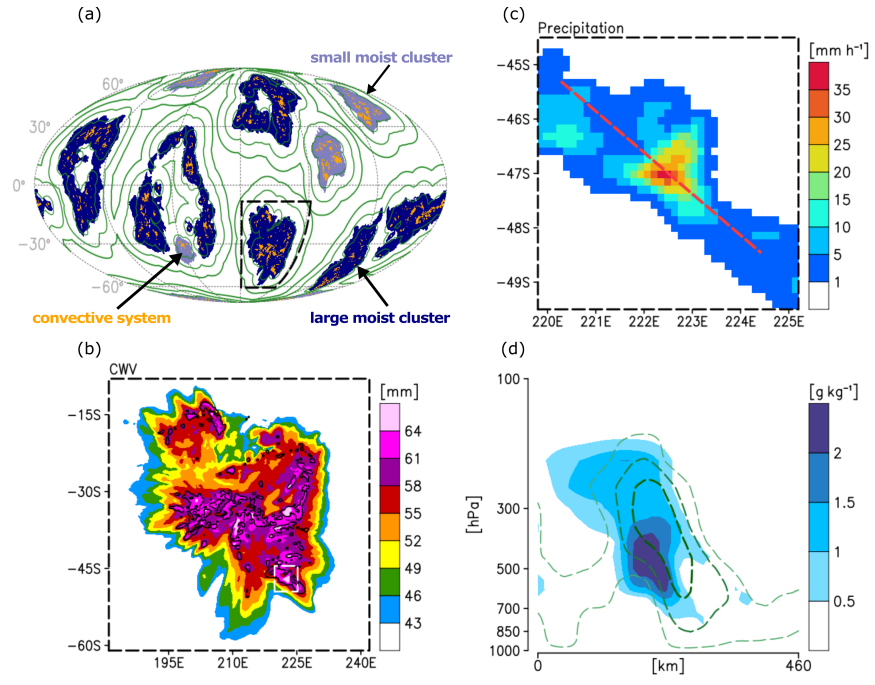
March 6, 2023

## Abstract

Observations suggest tropical convection intensifies when aerosol concentrations enhance, but quantitative estimations of this effect remain highly uncertain. Leading theories for explaining the intensification are based on the dynamical response of convection to changes in cloud microphysics independently from possible changes in the environment. Here, we provide a new perspective on aerosol indirect effects on tropical convection by using a global convection-permitting model that realistically simulates convection-circulation interaction. Simulations of radiative-convective equilibrium show that pollution facilitates the development of deep convection in a drier environment, but cloud condensates are more likely to be exported from moist clusters to dry areas, impeding the large-scale moisture-convection feedback and limiting the intensity of maximum precipitation (30 vs. 47 mm h<sup>-1</sup>). Our results emphasize the importance of allowing atmospheric phenomena to evolve continuously across spatial and temporal scales in simulations when investigating the response of tropical convection to changes in cloud microphysics.







1  
2  
3  
4  
5  
6  
7  
8  
9  
10  
11  
12  
13

# Modulation of Tropical Convection-circulation Interaction by Aerosol Indirect Effects in a Global Convection-permitting Model

Chun-Yian Su<sup>1,2</sup>, Chien-Ming Wu<sup>2</sup>, Wei-Ting Chen<sup>2</sup>, and John M. Peters<sup>1</sup>

<sup>1</sup>Department of Meteorology and Atmospheric Science, The Pennsylvania State University, University Park, PA

<sup>2</sup>Department of Atmospheric Sciences, National Taiwan University, Taipei city, Taiwan

## Key Points:

- Simulations of the global convection-permitting model provide a new perspective on aerosol indirect effects.
- Pollution facilitates the development of deep convection in a drier environment.
- The response of large-scale circulation to pollution limits the intensity of maximum precipitation.

---

Corresponding author: Chien-Ming Wu, [mog@as.ntu.edu.tw](mailto:mog@as.ntu.edu.tw)

## Abstract

Observations suggest tropical convection intensifies when aerosol concentrations enhance, but quantitative estimations of this effect remain highly uncertain. Leading theories for explaining the intensification are based on the dynamical response of convection to changes in cloud microphysics independently from possible changes in the environment. Here, we provide a new perspective on aerosol indirect effects on tropical convection by using a global convection-permitting model that realistically simulates convection-circulation interaction. Simulations of radiative-convective equilibrium show that pollution facilitates the development of deep convection in a drier environment, but cloud condensates are more likely to be exported from moist clusters to dry areas, impeding the large-scale moisture-convection feedback and limiting the intensity of maximum precipitation (30 vs. 47 mm h<sup>-1</sup>). Our results emphasize the importance of allowing atmospheric phenomena to evolve continuously across spatial and temporal scales in simulations when investigating the response of tropical convection to changes in cloud microphysics.

## Plain Language Summary

How does air pollution affect thunderstorm intensity over the tropical ocean? Past studies have proposed different opinions but generally neglect the interplay between the development of thunderstorms and the long-range movement of air that redistributes the Earth's thermal energy and moisture. Here, we address this question by investigating results from numerical experiments in which the global domain is used to simulate the response of individual thunderstorms and large-scale air motion to pollution. Our results show that tropical thunderstorms with given moisture are more vigorous under the polluted scenario. However, pollution makes the thunderstorms keep less moisture in their surroundings, limiting the maximum intensity of thunderstorms and weakening the large-scale air motion that supplies moisture to thunderstorms. Our results suggest that the interplay between the development of thunderstorms and the long-range movement of air is crucial in determining the effects of pollution in the tropical atmosphere.

## 1 Introduction

Deep convective clouds (DCCs) play a critical role in the global climate system via their role in the Earth's energy budget (Arakawa, 2004; Hartmann et al., 2001). They can aggregate into organized convective systems that span hundreds to a thousand kilometers (Houze, 2004) and contribute significantly to tropical rainfall (Chen et al., 2021; Houze et al., 2015; Nesbitt et al., 2006; Tao & Chern, 2017; Yuan & Houze, 2010). Observations suggest that updrafts of tropical DCCs can be invigorated by enhanced aerosol concentrations that arise from human activities and natural sources (Andreae et al., 2004; Koren et al., 2008; Niu & Li, 2012; Pan et al., 2021; Storer et al., 2014). By acting as cloud condensate nuclei (CCN) or ice nuclei (IN), aerosols change cloud properties by influencing cloud microphysics and dynamics, meanwhile influencing cloud-radiation feedbacks (i.e., aerosol indirect effects (AIEs); see reviews of Fan et al. (2016) and Tao et al. (2012)). A deeper understanding of AIEs on tropical DCCs and organized convective systems could improve the prediction of extreme precipitation events in global weather and climate models. However, the underlying mechanisms of how the updrafts are invigorated remain elusive and are often debated (Fan et al., 2018; Fan & Khain, 2021; W. W. Grabowski & Morrison, 2020, 2021; Igel & van den Heever, 2021). A particular challenge of understanding AIEs using observations is that the observed aerosol concentrations in the environments of DCCs often covary with other meteorological factors, such as convective available potential energy and vertical wind shear (W. W. Grabowski, 2018; Nishant & Sherwood, 2017; Varble, 2018), and the influences of meteorological and aerosol variability are difficult to disentangle from one another. Further, there is evidence from simulations that AIEs on DCCs vary as a function of meteorological conditions such as shear

64 and humidity (Fan et al., 2009; van den Heever & Cotton, 2007; Khain et al., 2008; Ko-  
65 ren et al., 2010; Z. Lebo, 2018), which further complicates our ability to isolate the aerosol  
66 effects from other meteorological processes. AIEs are underrepresented in global climate  
67 models because of these knowledge gaps, which contributes to considerable uncertainty  
68 in estimating human climate forcing (Forster et al., 2021).

69 To investigate the aerosol indirect effects on DCCs that interact with their surround-  
70 ing environment, Abbott and Cronin (2021) carried out simulations using a small do-  
71 main ( $128 \times 128 \text{ km}^2$ ) three-dimension cloud-resolving model (3-D CRM) with parame-  
72 terized large-scale dynamics under the weak temperature gradient (WTG) approxima-  
73 tion (Sobel et al., 2001). Abbott and Cronin (2021) suggested that enhanced CCN con-  
74 centrations produce clouds that mix more condensed water into the surrounding air. This  
75 enhances the environment favorably for subsequent convection by moistening the free  
76 troposphere and reducing the deleterious effects of entrainment. The humidity-entrainment  
77 mechanism they proposed is distinct from past work, which linked stronger updrafts with  
78 latent heat released by cloud condensation (Fan et al., 2018) or freezing (Rosenfeld et  
79 al., 2008) independently from possible changes in the environment. Anber et al. (2019)  
80 also used a small domain ( $192 \times 192 \text{ km}^2$ ) 3-D CRM with parameterized large-scale dy-  
81 namics to carry out simulations with different number concentrations of CCN but found  
82 a contrasting result. In their simulations, convection and mean precipitation get weaker  
83 when the CCN concentration increases. They suggested that the changes are associated  
84 with the modulation of coupling between convective processes and large-scale motions  
85 that overall reduces surface enthalpy fluxes.

86 Using a large domain ( $10000 \text{ km}$ ) two-dimension CRM configured in radiative-convective  
87 equilibrium (RCE; Manabe & Strickler, 1964), van den Heever et al. (2011) found a weak  
88 response of the large-scale organization of convection and the domain-averaged precip-  
89 itation to enhanced CCN concentrations. They suggested that AIEs on the three trop-  
90 ical cloud modes are opposite in sign, offsetting each other, thus producing a weak domain-  
91 wide response. In contrast, a more recent study by Beydoun and Hoose (2019) that used  
92 a large channel-shaped domain ( $2000 \times 120 \text{ km}^2$ ) 3-D CRM found a comparatively large  
93 decrease in domain-averaged precipitation in their RCE simulations with enhanced CCN  
94 concentrations. They suggested that enhanced CCN concentrations lead to the weak-  
95 ened large-scale organization of convection, increased midlevel and upper-level clouds,  
96 decreased radiative cooling, and decreased domain-averaged precipitation.

97 The difference in the above findings is likely influenced by the representation of large-  
98 scale dynamics and the geometry of the simulation domain, which could modulate convection-  
99 circulation interaction hence affect the overall AIEs. For example, a horizontal scale of  
100 the model domain larger than  $5000 \text{ km}$  was suggested to be large enough to represent  
101 the natural scale of large-scale organization of convection (Matsugishi & Satoh, 2022;  
102 Patrizio & Randall, 2019; Yanase et al., 2022). Advances in computational resources have  
103 allowed for global model simulations that explicitly simulate deep convection (Stevens  
104 et al., 2019). These global convection-permitting models have been applied to investi-  
105 gate how clouds and convective processes couple to large-scale circulation and determine  
106 cloud feedbacks and climate sensitivity (Wing et al., 2020). However, how is the coupling  
107 of DCCs and large-scale circulations affected by enhanced aerosol concentrations has not  
108 been fully understood.

109 This study aims to investigate the modulation of tropical convection-circulation in-  
110 teraction by AIEs in global simulations that simultaneously resolve the dynamical re-  
111 sponse of convection to changes in cloud microphysics and allow large-scale circulations  
112 to naturally develop since the horizontal scale is not artificially constrained by the do-  
113 main size or shape. The modulation of tropical convection-circulation interaction by AIEs  
114 is demonstrated by analyzing the responses of moisture distribution, convection struc-  
115 tures, and large-scale circulation to pollution. Section 2 introduces more details about

116 the model and the experiment design. Section 3 describes the results, and the summary  
 117 and discussion are presented in section 4.

## 118 2 Model Description and Experiment Design

119 We use the Central Weather Bureau Global Forecast System (CWBGFS; Su et al.,  
 120 2021a, 2021b; SU et al., 2022), which is a global convection-permitting model run at the  
 121 horizontal resolution of 15 km, to carry out our experiments. Deep convection in the CW-  
 122 BGFS is represented by the unified relaxed Arakawa-Schubert scheme (URAS; Su et al.,  
 123 2021b) in which the representation transitions from the parameterization to the explicit  
 124 simulation as the diagnosed convective updraft fraction increases (Arakawa & Wu, 2013;  
 125 Wu & Arakawa, 2014). Hence, the CWBGFS with the URAS can explicitly but efficiently  
 126 simulate deep convection and convection-circulation interaction on the global scale. This  
 127 model partially resolve circulations in organized convective systems and reproduce the  
 128 observed feature of convective systems that stronger extreme precipitation occurs in hor-  
 129 izontally larger systems (Hamada et al., 2014; SU et al., 2022).

130 The CWBGFS uses the two-moment Predicted Particle Properties bulk microphysics  
 131 scheme (P3; Morrison & Milbrandt, 2015) to represent cloud microphysical processes,  
 132 including cloud-aerosol interaction. The aerosol concentration prescribed in P3 is fixed  
 133 throughout the integration and acts as CCN. Cloud-aerosol interaction is not included  
 134 in the URAS. In our simulations, the averaged percentage of precipitation produced by  
 135 explicitly simulated convection is more than 93 % over precipitation events stronger than  
 136 5 mm h<sup>-1</sup>, indicating that most of the cloud-aerosol interactions associated with deep con-  
 137 vection are resolved. The rest of the descriptions regarding physics suites and the dy-  
 138 namic core of the CWBGFS can be found in Su et al. (2021a).

139 Two idealized non-rotating aqua-planet simulations configured in RCE are carried  
 140 out. Simulations in RCE have been extensively used to investigate feedback among clouds,  
 141 environmental moisture, radiation, and precipitation (Bretherton et al., 2005; Coppin  
 142 & Bony, 2015; Cronin & Wing, 2017; Emanuel et al., 2014; Holloway & Woolnough, 2016;  
 143 Pendergrass et al., 2016; Popke et al., 2013; Singh & O’Gorman, 2013, 2015; Wing & Emanuel,  
 144 2014; Wing et al., 2020), and therefore provide an ideal experimental setting to study  
 145 AIEs. Under certain circumstances, convection in RCE spontaneously self-organizes into  
 146 one or more moist ascending clusters surrounded by dry subsiding convection-free ar-  
 147 eas in simulations configured in non-rotating RCE (convective self-aggregation (CSA);  
 148 C. Muller et al., 2022; Wing et al., 2017). We note that CSA occurs in the simulations  
 149 of van den Heever et al. (2011) and Beydoun and Hoose (2019).

150 The simulations are initialized with an analytic sounding (Wing et al., 2018) that  
 151 approximates the moist tropical sounding of Dunion (2011), and the initial horizontal  
 152 winds are set to zero. The initial surface pressure of all grid columns is 1014.8 hPa. The  
 153 incoming solar radiation (409.6 W m<sup>-2</sup>), the sea surface temperature (300 K), and the  
 154 surface albedo (0.07) are spatially uniform and constant in time. The simulations are  
 155 run for 120 days, and the random perturbation of temperature from 0.1 to 0.02 K is added  
 156 to the five lowest model levels in the first 20 days to speed up convection initiation. The  
 157 only difference between the two simulations is the prescribed spatially uniform aerosol  
 158 number mixing ratio set in P3. They are set at  $3 \times 10^8$  kg<sup>-1</sup> and  $3 \times 10^{10}$  kg<sup>-1</sup>, represent-  
 159 ing the pristine and polluted scenarios, respectively. The scenarios here are referred to  
 160 the marine environment (Andreae, 2009) and the urban environment (Chang et al., 2021)  
 161 and are used to evaluate the upper bound of AIEs on convection-circulation interaction.  
 162 In the following section, 30 days of hourly output (days 90 to 120) are analyzed when  
 163 the simulation is in an RCE state.

164 The overall results of the pristine run are showcased in Fig. 1, demonstrating that  
 165 our simulations resemble the global model simulations in the RCE model intercompar-

166 ison project (Wing et al., 2018, 2020), in which convection self-organizing into multiple  
 167 moist clusters (Fig. 1a). Fig. 1b shows the spatial distribution of column water vapor  
 168 (CWV) of a moist cluster, indicating high heterogeneity that is coupled to spatial convec-  
 169 tion structures. Precipitation stronger than  $30 \text{ mm h}^{-1}$  (Fig. 1c) is found in a convec-  
 170 tive system with intense resolved updrafts ( $>1 \text{ m s}^{-1}$ ) (Fig. 1d). Fig. 1 with more detail  
 171 will be introduced in the following section.

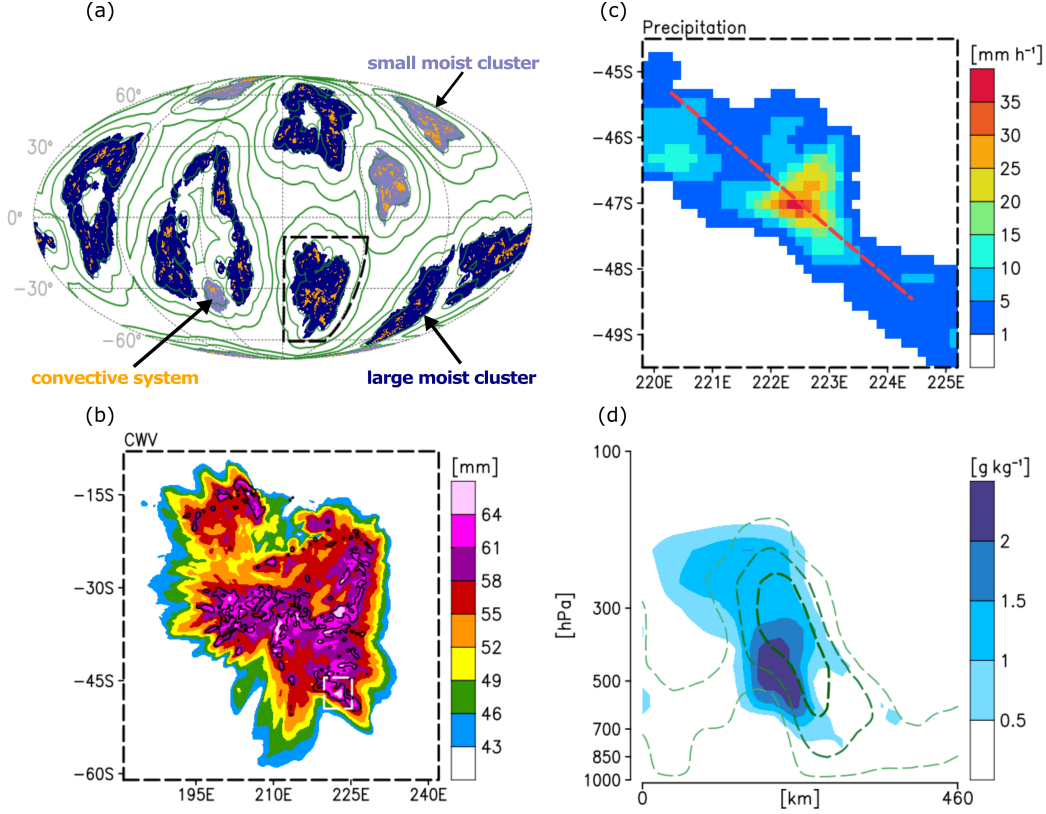


**Figure 1.** A snapshot of moist clusters smaller (light blue shaded) and larger (navy shaded) than 1000 km of horizontal scale, convective systems (orange shaded), and distance to the nearest convective system (green contours of 375, 1125, 1875 km) of the pristine run on day 106.5 (a). Column water vapor (mm) and convective systems (black contours) in a moist cluster (b), which the domain is demonstrated by the black dashed lines in (a). Precipitation intensity ( $\text{mm h}^{-1}$ ) of a convective system (c), which the domain is demonstrated by the white dashed lines in (b). The vertical profiles of mixed-phase cloud condensates (shaded) and vertical velocity (green contours of 0.1, 0.5,  $1 \text{ m s}^{-1}$ ) (d) along the red dashed line in (c). See the context for the definition of moist clusters and convective systems. The horizontal scale is determined by the square root of the cluster’s horizontal area.

172 **3 Results**

173 We start from demonstrating the response of moisture probability distribution to  
 174 enhanced CCN concentrations. In both runs, the distribution of CWV is bimodal (Fig.  
 175 2). The bimodality suggests the presence of an aggregated state (Arnold & Randall, 2015;  
 176 Tsai & Wu, 2017) which is maintained by large-scale circulation. The difference between  
 177 the two local maxima of the bimodality is smaller in the polluted run, suggesting AIEs

178 drive columns away from both moist and dry equilibria in the pristine run. We use the  
 179 CWV value that corresponds to the smallest value along the curve in Fig. 2 between the  
 180 local maxima at dry and moist CWV values as the threshold to define moist clusters (i.e.,  
 181 43 mm in both runs). The difference in area coverage percentage of moist clusters in the  
 182 global domain between the two runs is less than 3 %. The moist clusters in the polluted  
 183 run are notably drier than that in the pristine run. Further, the number of moist clusters  
 184 in the polluted run is 23 % more than that in the pristine run. Sixty-five percent  
 185 of moist clusters are smaller than 1000 km of horizontal scale in the polluted run, and  
 186 there are 45 % of them in the pristine run.

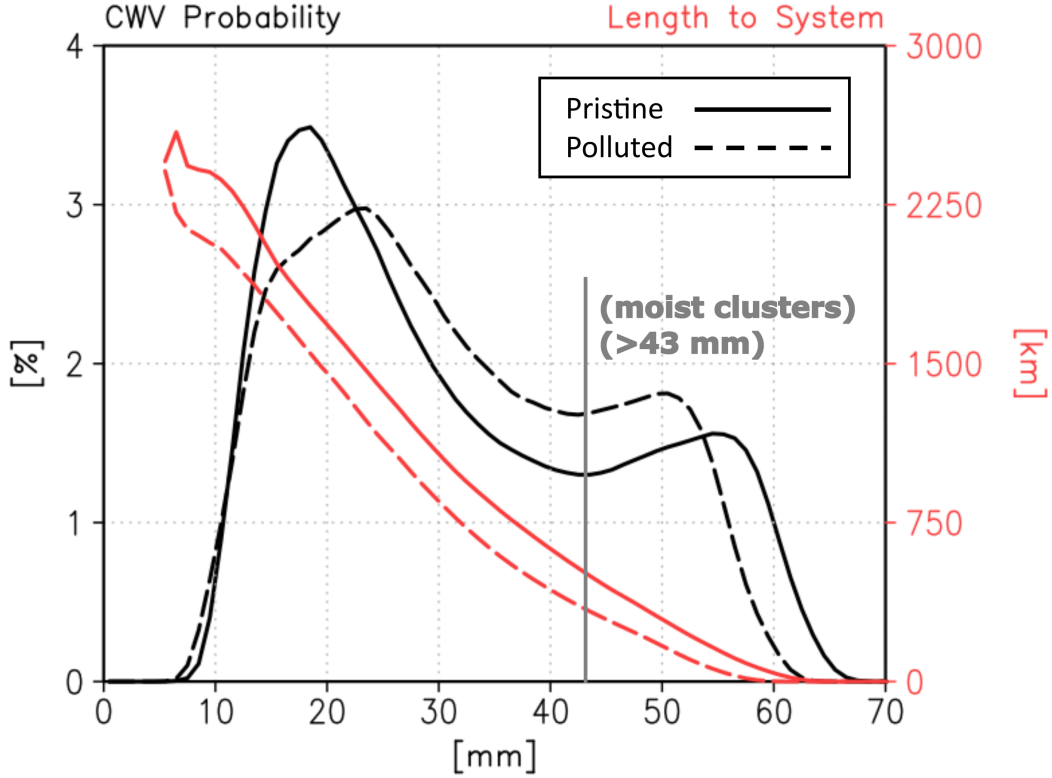


**Figure 2.** Probability distribution of column water vapor (black) and distance to the nearest convective system conditional sampled by column water vapor (red) from days 90 to 120. The gray line labels 43 mm of column water vapor, which is set as the criteria for defining a moist cluster.

187 We evaluate AIEs by first identifying the updraft regions of convective systems as  
 188 laterally connected columns of vertical velocity  $>0.1 \text{ m s}^{-1}$  in any level between 700 to  
 189 400 hPa (Fig. 1a-b). A critical characteristic of tropical deep moist convection is the rapid  
 190 intensification of precipitation once CWV has exceeded a critical value, which character-  
 191 izes the effect of water vapor on the buoyancy of clouds through entrainment (Bretherton  
 192 et al., 2004; Neelin et al., 2009; Peters & Neelin, 2006). Hence, we investigate the influ-  
 193 ence of pollution on this precipitation-CWV dependency. Analyses among all updraft  
 194 regions with a given CWV indicate that both of our simulations mimic the precipitation-  
 195 CWV dependency seen in nature, with a rapid increase in mixed-phase cloud condensate,  
 196 updraft intensity (Fig. 3a-b), and precipitation (Fig. 3c) occurring in both simu-  
 197 lations above a certain threshold in CWV. However, a distinct difference of the polluted  
 198 run from the pristine one is that the threshold CWV which heralds the increase in con-

199 vective intensity occurs at a lower CWV value (57 mm) than it does in the pristine run  
200 (62 mm).

201 Fig. 3a-b show that the vertical profiles to the right of the CWV thresholds resem-  
202 ble the convection structures of deep convection at the developing and mature stage, and  
203 the profiles to the left resemble deep convection at the dissipating stage, in which mixed-  
204 phase cloud condensates concentrate at mid-level free atmosphere beneath which weak  
205 downdrafts due to water loading take place. In the dissipating stage, moisture in the pol-  
206 luted run is more heavily distributed over the mid-to-low free atmosphere (Fig. 3d). The  
207 water vapor mixing ratio there is  $1.5 \text{ g kg}^{-1}$  more than that in the pristine run. The dif-  
208 ference may be caused by the stronger evaporation of raindrops as we found there is more  
209 mass but nearly the same number of falling raindrops beneath clouds in the polluted run  
210 leading to two times stronger surface precipitation (figure not shown). These raindrops  
211 could be from the melting of graupel and hail since the warm-rain process is suppressed  
212 due to pollution.

213 Past studies have shown that humidity in the lower free atmosphere is critical to  
214 the onset of tropical deep convection (Derbyshire et al., 2004; Holloway & Neelin, 2009,  
215 2010; Schiro et al., 2016; Tompkins, 2001). The enhanced moisture in the lower free at-  
216 mosphere increases the buoyancy of entraining plumes, leading to an increased chance  
217 of deep convection. The signal of the exceeding moisture in the mid-to-low free atmo-  
218 sphere in the polluted run extends to the CWV regimes of developing and mature con-  
219 vection (Fig. 3d), in which the increase in moisture in the mid-to-high atmosphere re-  
220 flects the prevalence of convection (Fig. 3a-b). The modulated moisture distribution, orig-  
221 inating from the response of dissipating stage of convection to changes in cloud micro-  
222 physics, enhances conditional instability, potentially contributing to the development of  
223 subsequent convection. Further investigations on the mechanism will be carried out in  
224 the future.

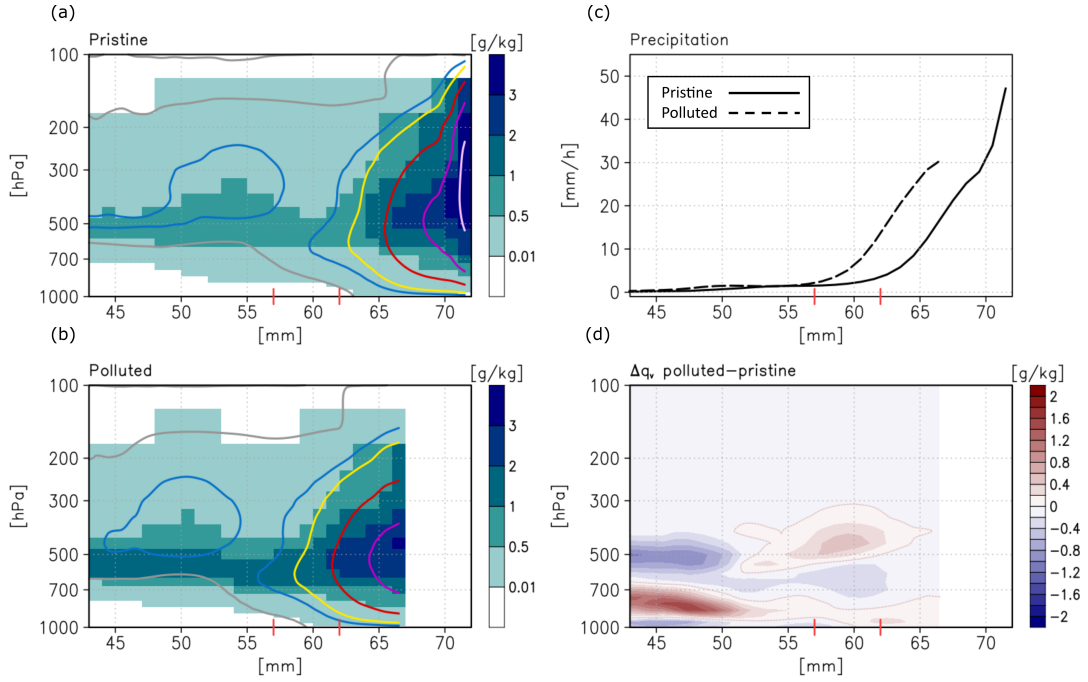


**Figure 3.** Mass mixing ratio of cloud water and cloud ice (shaded) and vertical velocity (contours at 0, 0.1, 0.2, 0.5, 1, 2  $\text{m s}^{-1}$ ) within the updraft regions of convective systems conditional sampled by column water vapor of the pristine (a) and the polluted (b) run from days 90 to 120. Precipitation intensity of the two runs (c) and the difference of water vapor mixing ratio (polluted run minus the pristine run) (d) sampled by the same method. The red dotted line in (d) shows the contour of  $0 \text{ g kg}^{-1}$ . The red sticks along the x-axis show the CWV value of 57 and 62 mm

225 However, the highest CWV environment over the updraft regions ( $>67 \text{ mm}$ ) in the  
 226 pristine run is absent in the polluted run (Fig. 3). The polluted run has notably drier  
 227 moist clusters (Fig. 2), leading to the weaker maximum intensity of updraft and precipi-  
 228 tation ( $30 \text{ vs. } 47 \text{ mm h}^{-1}$ ). As the moisture distribution is maintained by large-scale cir-  
 229 culation, we investigate the influence of pollution on large-scale circulation by sorting  
 230 the distance to the nearest convective system and projecting horizontal winds in the di-  
 231 rection pointing to the nearest system (green contours in Fig. 1a). Large-scale circula-  
 232 tion has often been visualized with a streamfunction in moisture space when analyzing  
 233 self-aggregated runs to RCE (Arnold & Putman, 2018; Bretherton et al., 2005; Holloway  
 234 & Woolnough, 2016; C. Muller & Bony, 2015; C. J. Muller & Held, 2012). The stream-  
 235 function analyzed in past studies is designed to investigate the energy transport between  
 236 dry areas and moist clusters but it does not represent circulation in physical space. It  
 237 is natural to analyze large-scale circulation in physical space when using a global convec-  
 238 tion-permitting model with an appropriate choice of the source of momentum and energy trans-  
 239 port. The result shows that both runs exhibit typical structures of tropical circulation,  
 240 including low-level inflow, mid-level outflow, and deep convection outflow (Johnson et  
 241 al., 1999), but every component of the circulation is weaker in the polluted run (Fig. 4).

242 We trace the cause of the weaker large-scale circulation down to the influence of  
 243 pollution on the geographical distribution of convective systems (i.e., updraft regions).  
 244 In the polluted run, convective systems develop geographically closer to the meander-  
 245 ing margin (i.e.,  $43 \text{ mm}$ ) of moist clusters, because CWV increases monotonically from  
 246 dry areas toward moist clusters (Fig. 1b), and convection strength enhances more rapidly

247 as CWV increases in the polluted run (Fig. 3b). Fig. 2 shows that the average distance  
 248 from the edges of moist clusters to the nearest convective system in the pristine run is  
 249 1.5 times longer than that in the polluted run. Meanwhile, inhibiting the warm-rain pro-  
 250 cess by pollution could increase the mid-level static stability as a result of a latent heat-  
 251 ing dipole associated with the freezing water and melting ice above and below the freez-  
 252 ing level. Previous studies suggested that an increase in mid-level static stability pro-  
 253 motes detrainment (Johnson et al., 1999; Patrizio & Randall, 2019; Posselt et al., 2008,  
 254 2012). Overall, cloud condensates in the polluted run are more likely to be exported from  
 255 moist clusters to dry areas rather than stay in moist clusters and then re-evaporate. The  
 256 export of clouds impedes the moisture-convective feedback in which moistening environ-  
 257 ment by convection plays a key role in favoring subsequent development of convection  
 258 (W. Grabowski & Moncrieff, 2004; Holloway & Neelin, 2009). The above inference is sup-  
 259 ported by Fig. 4b, which shows that the exceeding cloud condensates in the polluted run  
 260 coincide with the mid-level outflow of the large-scale circulation.

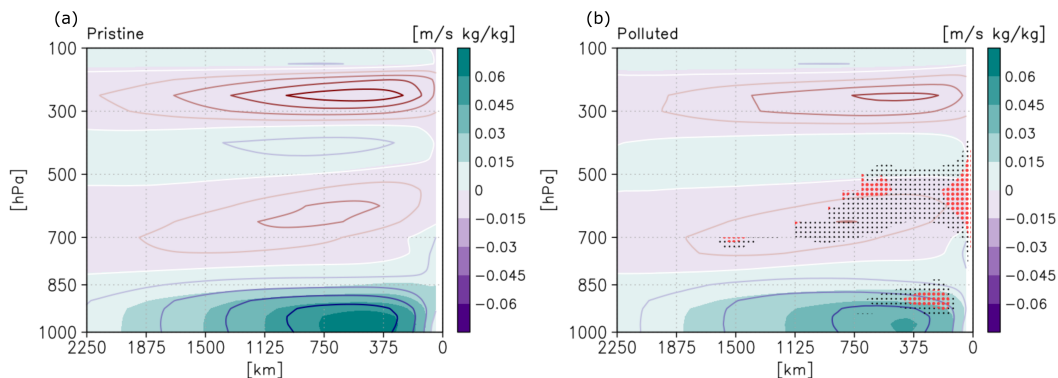


**Figure 4.** Water vapor flux (shaded) and horizontal winds (contours from  $-4$  to  $4$   $\text{m s}^{-1}$  with an interval of  $1$   $\text{m s}^{-1}$  using a color scale from maroon to white to navy) projected to the direction of pointing to the nearest convective system in the pristine (a) and the polluted (b) run from days 90 to 120. Positive values are vectors toward the system. The black and red dots in (b) show where the ratio of cloud water mixing ratio in the polluted run over the pristine one larger than 1 and 2, respectively

## 261 4 Summary and Discussion

262 This study investigates the response of tropical convection-circulation interaction  
 263 to enhanced CCN concentrations using non-rotating RCE simulations of a global convection-  
 264 permitting model run at 15 km horizontal resolution. Deep convection in the model is  
 265 represented in a way that the explicit simulation of convection seeds cloud-aerosol in-  
 266 teraction and is responsible for strong precipitation events. The simulations allow for the  
 267 large-scale organization of convection realistically inducing circulation without artificial  
 268 constraints of scale separation assumption, domain size, or domain shape. The novel find-  
 269 ing in this study is that pollution facilitates the development of deep convection in a drier  
 270 environment, while the response of large-scale circulation limits the intensity of maxi-  
 271 mum precipitation. Our results emphasize the importance of allowing atmospheric phe-  
 272 nomena to evolve continuously across spatial and temporal scales in simulations when  
 273 investigating the response of tropical convection to changes in cloud microphysics.

274 Connecting our result to the existing driving and maintaining mechanisms of CSA  
 275 could inspire future investigation on the response of global warming to varied CCN con-

276 concentrations since CSA is known to modulate climate sensitivity (Cronin & Wing, 2017).  
 277 The possible connections include:

- 278 1. The export of mid-level cloud condensates could weaken the radiatively driven sub-  
 279 sidence over the dry areas that drives CSA (Beydoun & Hoose, 2019; Bretherton  
 280 et al., 2005; C. J. Muller & Held, 2012; Wing & Emanuel, 2014; Holloway & Wool-  
 281 nough, 2016).
- 282 2. The response of cold pool dynamics to cloud microphysics has received consider-  
 283 able attention in the literature (Z. J. Lebo & Morrison, 2014; Seigel et al., 2013;  
 284 Storer et al., 2014; Su et al., 2020; Tao et al., 2007; van den Heever & Cotton, 2007).  
 285 Cold pools associated with the closer-to-edge convective systems in the polluted  
 286 run could mix low-level dry areas and moist clusters more effectively, weakening  
 287 the CSA (Jeevanjee & Romps, 2013; C. Muller & Bony, 2015).

288 Past studies (Arnold & Randall, 2015; Khairoutdinov & Emanuel, 2018) indicated  
 289 that the large-scale organization of convection (i.e., CSA) in non-rotating RCE simula-  
 290 tions and MJO-like (i.e., Madden-Julian Oscillation; Madden & Julian, 1971) disturbance  
 291 in rotating RCE simulations share the same driving mechanism (i.e., cloud-radiation feed-  
 292 backs) in which AIEs can be critical. One of the characteristics of MJO propagation is  
 293 that MJOs suffer from a barrier effect when it propagates over the Maritime Continent  
 294 (MC) (Kim et al., 2014; Zhang & Ling, 2017). The development of convective systems  
 295 over the water in the MC region plays a crucial role in carrying the MJO signal through  
 296 the MC (Ling et al., 2019). Around the globe, MC is a major source of different types  
 297 of aerosol (Reid et al., 2012; Salinas et al., 2013; Shpund et al., 2019). The modulation  
 298 of the size of moist clusters and the geographical distribution of convective systems by  
 299 enhanced CCN concentrations potentially provides a new perspective on the existing MJO  
 300 theories (Jiang et al., 2020; Zhang, 2013). A possible approach for the investigation is  
 301 to evaluate sub-seasonal hindcasts of an active MJO event with different aerosol emis-  
 302 sion scenarios.

## 303 5 Open Research

304 The model output data of a temporal snapshot, the Fortran program that computes  
 305 vertical atmospheric profiles conditional sampled by column water vapor and the distance  
 306 to the nearest convective system, and the GrADS plotting scripts in this study are avail-  
 307 able at <https://doi.org/10.6084/m9.figshare.22149617.v1>.

## 308 Acknowledgments

309 Chien-Ming Wu and Chun-Yian Su's efforts were supported by National Science and Tech-  
 310 nology Council (NSTC) in Taiwan grant 111-2111-M-002-012-NSTC. Wei-Ting Chen was  
 311 supported by Ministry of Science and Technology (MOST) in Taiwan grant 109-2628-  
 312 M-002-003-MY3. J. Peters was supported by National Science Foundation (NSF) grants  
 313 AGS-1928666, AGS-1841674, and the Department of Energy Atmospheric System Re-  
 314 search (DOE ASR) grant DE-SC0000246356. We thank Dr. Jen-Her Chen in Central  
 315 Weather Bureau for his support of this work.

## 316 References

- 317 Abbott, T. H., & Cronin, T. W. (2021, January). Aerosol invigoration of atmo-  
 318 spheric convection through increases in humidity. *Science*, *371*(6524), 83–85.  
 319 Retrieved from <https://doi.org/10.1126/science.abc5181> doi: 10.1126/  
 320 science.abc5181
- 321 Anber, U. M., Wang, S., Gentine, P., & Jensen, M. P. (2019, September). Prob-  
 322 ing the response of tropical deep convection to aerosol perturbations using

- 323 idealized cloud-resolving simulations with parameterized large-scale dynam-  
 324 ics. *Journal of the Atmospheric Sciences*, 76(9), 2885–2897. Retrieved from  
 325 <https://doi.org/10.1175/jas-d-18-0351.1> doi: 10.1175/jas-d-18-0351.1
- 326 Andreae, M. O. (2009, January). Correlation between cloud condensation nuclei  
 327 concentration and aerosol optical thickness in remote and polluted regions. *At-*  
 328 *mospheric Chemistry and Physics*, 9(2), 543–556. Retrieved from [https://doi](https://doi.org/10.5194/acp-9-543-2009)  
 329 [.org/10.5194/acp-9-543-2009](https://doi.org/10.5194/acp-9-543-2009) doi: 10.5194/acp-9-543-2009
- 330 Andreae, M. O., Rosenfeld, D., Artaxo, P., Costa, A. A., Frank, G. P., Longo,  
 331 K. M., & Silva-Dias, M. A. F. (2004, February). Smoking rain clouds over the  
 332 amazon. *Science*, 303(5662), 1337–1342. Retrieved from [https://doi.org/](https://doi.org/10.1126/science.1092779)  
 333 [10.1126/science.1092779](https://doi.org/10.1126/science.1092779) doi: 10.1126/science.1092779
- 334 Arakawa, A. (2004, July). The cumulus parameterization problem: Past, present,  
 335 and future. *Journal of Climate*, 17(13), 2493–2525. Retrieved from  
 336 [https://doi.org/10.1175/1520-0442\(2004\)017<2493:ratcpp>2.0.co;2](https://doi.org/10.1175/1520-0442(2004)017<2493:ratcpp>2.0.co;2)  
 337 doi: 10.1175/1520-0442(2004)017(2493:ratcpp)2.0.co;2
- 338 Arakawa, A., & Wu, C.-M. (2013, July). A unified representation of deep moist  
 339 convection in numerical modeling of the atmosphere. part i. *Journal of the At-*  
 340 *mospheric Sciences*, 70(7), 1977–1992. Retrieved from [https://doi.org/10](https://doi.org/10.1175/jas-d-12-0330.1)  
 341 [.1175/jas-d-12-0330.1](https://doi.org/10.1175/jas-d-12-0330.1) doi: 10.1175/jas-d-12-0330.1
- 342 Arnold, N. P., & Putman, W. M. (2018, April). Nonrotating convective self-  
 343 aggregation in a limited area AGCM. *Journal of Advances in Modeling Earth*  
 344 *Systems*, 10(4), 1029–1046. Retrieved from [https://doi.org/10.1002/](https://doi.org/10.1002/2017ms001218)  
 345 [2017ms001218](https://doi.org/10.1002/2017ms001218) doi: 10.1002/2017ms001218
- 346 Arnold, N. P., & Randall, D. A. (2015, October). Global-scale convective aggre-  
 347 gation: Implications for the madden-julian oscillation. *Journal of Advances in*  
 348 *Modeling Earth Systems*, 7(4), 1499–1518. Retrieved from [https://doi.org/](https://doi.org/10.1002/2015ms000498)  
 349 [10.1002/2015ms000498](https://doi.org/10.1002/2015ms000498) doi: 10.1002/2015ms000498
- 350 Beydoun, H., & Hoose, C. (2019, April). Aerosol-cloud-precipitation interactions  
 351 in the context of convective self-aggregation. *Journal of Advances in Modeling*  
 352 *Earth Systems*, 11(4), 1066–1087. Retrieved from [https://doi.org/10.1029/](https://doi.org/10.1029/2018ms001523)  
 353 [2018ms001523](https://doi.org/10.1029/2018ms001523) doi: 10.1029/2018ms001523
- 354 Bretherton, C. S., Blossey, P. N., & Khairoutdinov, M. (2005, December). An  
 355 energy-balance analysis of deep convective self-aggregation above uniform SST.  
 356 *Journal of the Atmospheric Sciences*, 62(12), 4273–4292. Retrieved from  
 357 <https://doi.org/10.1175/jas3614.1> doi: 10.1175/jas3614.1
- 358 Bretherton, C. S., Peters, M. E., & Back, L. E. (2004, April). Relationships be-  
 359 tween water vapor path and precipitation over the tropical oceans. *Jour-*  
 360 *nal of Climate*, 17(7), 1517–1528. Retrieved from [https://doi.org/](https://doi.org/10.1175/1520-0442(2004)017<1517:rbwvpa>2.0.co;2)  
 361 [10.1175/1520-0442\(2004\)017<1517:rbwvpa>2.0.co;2](https://doi.org/10.1175/1520-0442(2004)017<1517:rbwvpa>2.0.co;2)  
 362 doi: 10.1175/1520-0442(2004)017(1517:rbwvpa)2.0.co;2
- 363 Chang, Y.-H., Chen, W.-T., Wu, C.-M., Moseley, C., & Wu, C.-C. (2021, Novem-  
 364 ber). Tracking the influence of cloud condensation nuclei on summer diurnal  
 365 precipitating systems over complex topography in taiwan. *Atmospheric Chem-*  
 366 *istry and Physics*, 21(22), 16709–16725. Retrieved from [https://doi.org/](https://doi.org/10.5194/acp-21-16709-2021)  
 367 [10.5194/acp-21-16709-2021](https://doi.org/10.5194/acp-21-16709-2021) doi: 10.5194/acp-21-16709-2021
- 368 Chen, P.-J., Chen, W.-T., Wu, C.-M., & Yo, T.-S. (2021, May). Convective cloud  
 369 regimes from a classification of object-based CloudSat observations over asian-  
 370 australian monsoon areas. *Geophysical Research Letters*, 48(10). Retrieved  
 371 from <https://doi.org/10.1029/2021gl092733> doi: 10.1029/2021gl092733
- 372 Coppin, D., & Bony, S. (2015, December). Physical mechanisms controlling the  
 373 initiation of convective self-aggregation in a general circulation model. *Jour-*  
 374 *nal of Advances in Modeling Earth Systems*, 7(4), 2060–2078. Retrieved from  
 375 <https://doi.org/10.1002/2015ms000571> doi: 10.1002/2015ms000571
- 376 Cronin, T. W., & Wing, A. A. (2017, December). Clouds, circulation, and climate  
 377 sensitivity in a radiative-convective equilibrium channel model. *Journal of Ad-*

- 378 *vances in Modeling Earth Systems*, 9(8), 2883–2905. Retrieved from [https://](https://doi.org/10.1002/2017ms001111)  
379 [doi.org/10.1002/2017ms001111](https://doi.org/10.1002/2017ms001111) doi: 10.1002/2017ms001111
- 380 Derbyshire, S., Beau, I., Bechtold, P., Grandpeix, J.-Y., Piriou, J.-M., Redelsperger,  
381 J.-L., & Soares, P. (2004, October). Sensitivity of moist convection to envi-  
382 ronmental humidity. *Quarterly Journal of the Royal Meteorological Society*,  
383 130(604), 3055–3079. Retrieved from <https://doi.org/10.1256/qj.03.130>  
384 doi: 10.1256/qj.03.130
- 385 Dunion, J. P. (2011, February). Rewriting the climatology of the tropical north  
386 atlantic and caribbean sea atmosphere. *Journal of Climate*, 24(3), 893–  
387 908. Retrieved from <https://doi.org/10.1175/2010jcli3496.1> doi:  
388 10.1175/2010jcli3496.1
- 389 Emanuel, K., Wing, A. A., & Vincent, E. M. (2014, February). Radiative-  
390 convective instability. *Journal of Advances in Modeling Earth Systems*, 6(1),  
391 75–90. Retrieved from <https://doi.org/10.1002/2013ms000270> doi:  
392 10.1002/2013ms000270
- 393 Fan, J., & Khain, A. (2021, January). Comments on “do ultrafine cloud condensa-  
394 tion nuclei invigorate deep convection?”. *Journal of the Atmospheric Sciences*,  
395 78(1), 329–339. Retrieved from <https://doi.org/10.1175/jas-d-20-0218.1>  
396 doi: 10.1175/jas-d-20-0218.1
- 397 Fan, J., Rosenfeld, D., Zhang, Y., Giangrande, S. E., Li, Z., Machado, L. A. T.,  
398 ... de Souza, R. A. F. (2018, January). Substantial convection and pre-  
399 cipitation enhancements by ultrafine aerosol particles. *Science*, 359(6374),  
400 411–418. Retrieved from <https://doi.org/10.1126/science.aan8461> doi:  
401 10.1126/science.aan8461
- 402 Fan, J., Wang, Y., Rosenfeld, D., & Liu, X. (2016, October). Review of  
403 aerosol–cloud interactions: Mechanisms, significance, and challenges. *Jour-  
404 nal of the Atmospheric Sciences*, 73(11), 4221–4252. Retrieved from  
405 <https://doi.org/10.1175/jas-d-16-0037.1> doi: 10.1175/jas-d-16-0037.1
- 406 Fan, J., Yuan, T., Comstock, J. M., Ghan, S., Khain, A., Leung, L. R., ... Ovchin-  
407 nikov, M. (2009, November). Dominant role by vertical wind shear in regulat-  
408 ing aerosol effects on deep convective clouds. *Journal of Geophysical Research*,  
409 114(D22). Retrieved from <https://doi.org/10.1029/2009jd012352> doi:  
410 10.1029/2009jd012352
- 411 Forster, P., Storelvmo, T., Armour, K., Collins, W., Dufresne, J.-L., Frame, D., ...  
412 Zhang, H. (2021). The earth’s energy budget, climate feedbacks, and cli-  
413 mate sensitivity [Book Section]. In V. Masson-Delmotte et al. (Eds.), *Climate  
414 change 2021: The physical science basis. contribution of working group i to  
415 the sixth assessment report of the intergovernmental panel on climate change*  
416 (p. 923–1054). Cambridge, United Kingdom and New York, NY, USA: Cam-  
417 bridge University Press. doi: 10.1017/9781009157896.009
- 418 Grabowski, W., & Moncrieff, M. (2004, October). Moisture–convection feedback in  
419 the tropics. *Quarterly Journal of the Royal Meteorological Society*, 130(604),  
420 3081–3104. Retrieved from <https://doi.org/10.1256/qj.03.135> doi: 10.  
421 1256/qj.03.135
- 422 Grabowski, W. W. (2018, October). Can the impact of aerosols on deep convec-  
423 tion be isolated from meteorological effects in atmospheric observations? *Jour-  
424 nal of the Atmospheric Sciences*, 75(10), 3347–3363. Retrieved from [https://](https://doi.org/10.1175/jas-d-18-0105.1)  
425 [doi.org/10.1175/jas-d-18-0105.1](https://doi.org/10.1175/jas-d-18-0105.1) doi: 10.1175/jas-d-18-0105.1
- 426 Grabowski, W. W., & Morrison, H. (2020, July). Do ultrafine cloud condensation  
427 nuclei invigorate deep convection? *Journal of the Atmospheric Sciences*, 77(7),  
428 2567–2583. Retrieved from <https://doi.org/10.1175/jas-d-20-0012.1> doi:  
429 10.1175/jas-d-20-0012.1
- 430 Grabowski, W. W., & Morrison, H. (2021, January). Reply to “comments on ‘do ul-  
431 trafine cloud condensation nuclei invigorate deep convection?’”. *Journal of the  
432 Atmospheric Sciences*, 78(1), 341–350. Retrieved from <https://doi.org/10>

- 433 .1175/jas-d-20-0315.1 doi: 10.1175/jas-d-20-0315.1
- 434 Hamada, A., Murayama, Y., & Takayabu, Y. N. (2014, October). Regional charac-  
 435 teristics of extreme rainfall extracted from TRMM PR measurements. *Journal*  
 436 *of Climate*, 27(21), 8151–8169. Retrieved from [https://doi.org/10.1175/](https://doi.org/10.1175/jcli-d-14-00107.1)  
 437 [jcli-d-14-00107.1](https://doi.org/10.1175/jcli-d-14-00107.1) doi: 10.1175/jcli-d-14-00107.1
- 438 Hartmann, D. L., Moy, L. A., & Fu, Q. (2001, December). Tropical convection and  
 439 the energy balance at the top of the atmosphere. *Journal of Climate*, 14(24),  
 440 4495–4511. Retrieved from [https://doi.org/10.1175/1520-0442\(2001\)](https://doi.org/10.1175/1520-0442(2001)014<4495:tcateb>2.0.co;2)  
 441 [014<4495:tcateb>2.0.co;2](https://doi.org/10.1175/1520-0442(2001)014<4495:tcateb>2.0.co;2) doi: 10.1175/1520-0442(2001)014<4495:  
 442 [tcateb>2.0.co;2](https://doi.org/10.1175/1520-0442(2001)014<4495:tcateb>2.0.co;2)
- 443 Holloway, C. E., & Neelin, J. D. (2009, June). Moisture vertical structure, col-  
 444 umn water vapor, and tropical deep convection. *Journal of the Atmospheric*  
 445 *Sciences*, 66(6), 1665–1683. Retrieved from [https://doi.org/10.1175/](https://doi.org/10.1175/2008jas2806.1)  
 446 [2008jas2806.1](https://doi.org/10.1175/2008jas2806.1) doi: 10.1175/2008jas2806.1
- 447 Holloway, C. E., & Neelin, J. D. (2010, April). Temporal relations of column water  
 448 vapor and tropical precipitation. *Journal of the Atmospheric Sciences*, 67(4),  
 449 1091–1105. Retrieved from <https://doi.org/10.1175/2009jas3284.1> doi:  
 450 [10.1175/2009jas3284.1](https://doi.org/10.1175/2009jas3284.1)
- 451 Holloway, C. E., & Woolnough, S. J. (2016, February). The sensitivity of convective  
 452 aggregation to diabatic processes in idealized radiative-convective equilib-  
 453 rium simulations. *Journal of Advances in Modeling Earth Systems*, 8(1),  
 454 166–195. Retrieved from <https://doi.org/10.1002/2015ms000511> doi:  
 455 [10.1002/2015ms000511](https://doi.org/10.1002/2015ms000511)
- 456 Houze, R. A. (2004, December). Mesoscale convective systems. *Reviews of Geo-*  
 457 *physics*, 42(4). Retrieved from <https://doi.org/10.1029/2004rg000150>  
 458 doi: 10.1029/2004rg000150
- 459 Houze, R. A., Rasmussen, K. L., Zuluaga, M. D., & Brodzik, S. R. (2015, Septem-  
 460 ber). The variable nature of convection in the tropics and subtropics: A legacy  
 461 of 16 years of the tropical rainfall measuring mission satellite. *Reviews of*  
 462 *Geophysics*, 53(3), 994–1021. Retrieved from [https://doi.org/10.1002/](https://doi.org/10.1002/2015rg000488)  
 463 [2015rg000488](https://doi.org/10.1002/2015rg000488) doi: 10.1002/2015rg000488
- 464 Igel, A. L., & van den Heever, S. C. (2021, August). Invigoration or enervation of  
 465 convective clouds by aerosols? *Geophysical Research Letters*, 48(16). Retrieved  
 466 from <https://doi.org/10.1029/2021gl093804> doi: 10.1029/2021gl093804
- 467 Jeevanjee, N., & Romps, D. M. (2013, March). Convective self-aggregation, cold  
 468 pools, and domain size. *Geophysical Research Letters*, 40(5), 994–998. Re-  
 469 trieved from <https://doi.org/10.1002/grl.50204> doi: 10.1002/grl.50204
- 470 Jiang, X., Adames, Á. F., Kim, D., Maloney, E. D., Lin, H., Kim, H., . . . Klinga-  
 471 man, N. P. (2020, August). Fifty years of research on the madden-julian  
 472 oscillation: Recent progress, challenges, and perspectives. *Journal of Geo-*  
 473 *physical Research: Atmospheres*, 125(17). Retrieved from [https://doi.org/](https://doi.org/10.1029/2019jd030911)  
 474 [10.1029/2019jd030911](https://doi.org/10.1029/2019jd030911) doi: 10.1029/2019jd030911
- 475 Johnson, R. H., Rickenbach, T. M., Rutledge, S. A., Ciesielski, P. E., & Schu-  
 476 bert, W. H. (1999, August). Trimodal characteristics of tropical convec-  
 477 tion. *Journal of Climate*, 12(8), 2397–2418. Retrieved from [https://](https://doi.org/10.1175/1520-0442(1999)012<2397:tcotc>2.0.co;2)  
 478 [doi.org/10.1175/1520-0442\(1999\)012<2397:tcotc>2.0.co;2](https://doi.org/10.1175/1520-0442(1999)012<2397:tcotc>2.0.co;2) doi:  
 479 [10.1175/1520-0442\(1999\)012<2397:tcotc>2.0.co;2](https://doi.org/10.1175/1520-0442(1999)012<2397:tcotc>2.0.co;2)
- 480 Khain, A. P., BenMoshe, N., & Pokrovsky, A. (2008, June). Factors determining the  
 481 impact of aerosols on surface precipitation from clouds: An attempt at classifi-  
 482 cation. *Journal of the Atmospheric Sciences*, 65(6), 1721–1748. Retrieved from  
 483 <https://doi.org/10.1175/2007jas2515.1> doi: 10.1175/2007jas2515.1
- 484 Khairoutdinov, M. F., & Emanuel, K. (2018, December). Intraseasonal variability in  
 485 a cloud-permitting near-global equatorial aquaplanet model. *Journal of the At-*  
 486 *mospheric Sciences*, 75(12), 4337–4355. Retrieved from [https://doi.org/10](https://doi.org/10.1175/jas-d-18-0152.1)  
 487 [.1175/jas-d-18-0152.1](https://doi.org/10.1175/jas-d-18-0152.1) doi: 10.1175/jas-d-18-0152.1

- 488 Kim, D., Kug, J.-S., & Sobel, A. H. (2014, January). Propagating versus non-  
 489 propagating madden–julian oscillation events. *Journal of Climate*, *27*(1),  
 490 111–125. Retrieved from <https://doi.org/10.1175/jcli-d-13-00084.1>  
 491 doi: 10.1175/jcli-d-13-00084.1
- 492 Koren, I., Feingold, G., & Remer, L. A. (2010, September). The invigoration  
 493 of deep convective clouds over the atlantic: aerosol effect, meteorology or  
 494 retrieval artifact? *Atmospheric Chemistry and Physics*, *10*(18), 8855–  
 495 8872. Retrieved from <https://doi.org/10.5194/acp-10-8855-2010> doi:  
 496 10.5194/acp-10-8855-2010
- 497 Koren, I., Martins, J. V., Remer, L. A., & Afargan, H. (2008, August). Smoke invig-  
 498 oration versus inhibition of clouds over the amazon. *Science*, *321*(5891), 946–  
 499 949. Retrieved from <https://doi.org/10.1126/science.1159185> doi: 10  
 500 .1126/science.1159185
- 501 Lebo, Z. (2018, February). A numerical investigation of the potential effects of  
 502 aerosol-induced warming and updraft width and slope on updraft intensity  
 503 in deep convective clouds. *Journal of the Atmospheric Sciences*, *75*(2), 535–  
 504 554. Retrieved from <https://doi.org/10.1175/jas-d-16-0368.1> doi:  
 505 10.1175/jas-d-16-0368.1
- 506 Lebo, Z. J., & Morrison, H. (2014, March). Dynamical effects of aerosol perturba-  
 507 tions on simulated idealized squall lines. *Monthly Weather Review*, *142*(3),  
 508 991–1009. Retrieved from <https://doi.org/10.1175/mwr-d-13-00156.1>  
 509 doi: 10.1175/mwr-d-13-00156.1
- 510 Ling, J., Zhang, C., Joyce, R., ping Xie, P., & Chen, G. (2019, March). Possible role  
 511 of the diurnal cycle in land convection in the barrier effect on the MJO by the  
 512 maritime continent. *Geophysical Research Letters*, *46*(5), 3001–3011. Retrieved  
 513 from <https://doi.org/10.1029/2019gl081962> doi: 10.1029/2019gl081962
- 514 Madden, R. A., & Julian, P. R. (1971, July). Detection of a 40–50 day oscillation  
 515 in the zonal wind in the tropical pacific. *Journal of the Atmospheric Sciences*,  
 516 *28*(5), 702–708. Retrieved from [https://doi.org/10.1175/1520-0469\(1971\)  
 517 028<0702:doadoi>2.0.co;2](https://doi.org/10.1175/1520-0469(1971)028<0702:doadoi>2.0.co;2) doi: 10.1175/1520-0469(1971)028<0702:doadoi>2  
 518 .0.co;2
- 519 Manabe, S., & Strickler, R. F. (1964, July). Thermal equilibrium of the atmosphere  
 520 with a convective adjustment. *Journal of the Atmospheric Sciences*, *21*(4),  
 521 361–385. Retrieved from [https://doi.org/10.1175/1520-0469\(1964\)  
 522 021<0361:teotaw>2.0.co;2](https://doi.org/10.1175/1520-0469(1964)021<0361:teotaw>2.0.co;2) doi: 10.1175/1520-0469(1964)021<0361:  
 523 teotaw>2.0.co;2
- 524 Matsugishi, S., & Satoh, M. (2022, May). Sensitivity of the horizontal scale  
 525 of convective self-aggregation to sea surface temperature in radiative con-  
 526 vective equilibrium experiments using a global nonhydrostatic model.  
 527 *Journal of Advances in Modeling Earth Systems*, *14*(5). Retrieved from  
 528 <https://doi.org/10.1029/2021ms002636> doi: 10.1029/2021ms002636
- 529 Morrison, H., & Milbrandt, J. A. (2015, January). Parameterization of cloud micro-  
 530 physics based on the prediction of bulk ice particle properties. part i: Scheme  
 531 description and idealized tests. *Journal of the Atmospheric Sciences*, *72*(1),  
 532 287–311. Retrieved from <https://doi.org/10.1175/jas-d-14-0065.1> doi:  
 533 10.1175/jas-d-14-0065.1
- 534 Muller, C., & Bony, S. (2015, July). What favors convective aggregation and why?  
 535 *Geophysical Research Letters*, *42*(13), 5626–5634. Retrieved from [https://doi  
 536 .org/10.1002/2015gl064260](https://doi.org/10.1002/2015gl064260) doi: 10.1002/2015gl064260
- 537 Muller, C., Yang, D., Craig, G., Cronin, T., Fildier, B., Haerter, J. O., ... Sher-  
 538 wood, S. C. (2022, January). Spontaneous aggregation of convective  
 539 storms. *Annual Review of Fluid Mechanics*, *54*(1), 133–157. Retrieved  
 540 from <https://doi.org/10.1146/annurev-fluid-022421-011319> doi:  
 541 10.1146/annurev-fluid-022421-011319
- 542 Muller, C. J., & Held, I. M. (2012, August). Detailed investigation of the self-

- 543 aggregation of convection in cloud-resolving simulations. *Journal of the At-*  
 544 *mospheric Sciences*, 69(8), 2551–2565. Retrieved from [https://doi.org/](https://doi.org/10.1175/jas-d-11-0257.1)  
 545 [10.1175/jas-d-11-0257.1](https://doi.org/10.1175/jas-d-11-0257.1) doi: 10.1175/jas-d-11-0257.1
- 546 Neelin, J. D., Peters, O., & Hales, K. (2009, August). The transition to strong con-  
 547 vection. *Journal of the Atmospheric Sciences*, 66(8), 2367–2384. Retrieved  
 548 from <https://doi.org/10.1175/2009jas2962.1> doi: 10.1175/2009jas2962  
 549 .1
- 550 Nesbitt, S. W., Cifelli, R., & Rutledge, S. A. (2006, October). Storm morphology  
 551 and rainfall characteristics of TRMM precipitation features. *Monthly Weather*  
 552 *Review*, 134(10), 2702–2721. Retrieved from [https://doi.org/10.1175/](https://doi.org/10.1175/mwr3200.1)  
 553 [mwr3200.1](https://doi.org/10.1175/mwr3200.1) doi: 10.1175/mwr3200.1
- 554 Nishant, N., & Sherwood, S. C. (2017, June). A cloud-resolving model study of  
 555 aerosol-cloud correlation in a pristine maritime environment. *Geophysical*  
 556 *Research Letters*, 44(11), 5774–5781. Retrieved from [https://doi.org/](https://doi.org/10.1002/2017gl073267)  
 557 [10.1002/2017gl073267](https://doi.org/10.1002/2017gl073267) doi: 10.1002/2017gl073267
- 558 Niu, F., & Li, Z. (2012, September). Systematic variations of cloud top tempera-  
 559 ture and precipitation rate with aerosols over the global tropics. *Atmospheric*  
 560 *Chemistry and Physics*, 12(18), 8491–8498. Retrieved from [https://doi.org/](https://doi.org/10.5194/acp-12-8491-2012)  
 561 [10.5194/acp-12-8491-2012](https://doi.org/10.5194/acp-12-8491-2012) doi: 10.5194/acp-12-8491-2012
- 562 Pan, Z., Rosenfeld, D., Zhu, Y., Mao, F., Gong, W., Zang, L., & Lu, X. (2021,  
 563 May). Observational quantification of aerosol invigoration for deep convective  
 564 cloud lifecycle properties based on geostationary satellite. *Journal of Geo-*  
 565 *physical Research: Atmospheres*, 126(9). Retrieved from [https://doi.org/](https://doi.org/10.1029/2020jd034275)  
 566 [10.1029/2020jd034275](https://doi.org/10.1029/2020jd034275) doi: 10.1029/2020jd034275
- 567 Patrizio, C. R., & Randall, D. A. (2019, July). Sensitivity of convective self-  
 568 aggregation to domain size. *Journal of Advances in Modeling Earth Systems*,  
 569 11(7), 1995–2019. Retrieved from <https://doi.org/10.1029/2019ms001672>  
 570 doi: 10.1029/2019ms001672
- 571 Pendergrass, A. G., Reed, K. A., & Medeiros, B. (2016, November). The link be-  
 572 tween extreme precipitation and convective organization in a warming climate:  
 573 Global radiative-convective equilibrium simulations. *Geophysical Research Let-*  
 574 *ters*, 43(21). Retrieved from <https://doi.org/10.1002/2016gl071285> doi:  
 575 [10.1002/2016gl071285](https://doi.org/10.1002/2016gl071285)
- 576 Peters, O., & Neelin, J. D. (2006, May). Critical phenomena in atmospheric precip-  
 577 itation. *Nature Physics*, 2(6), 393–396. Retrieved from [https://doi.org/10](https://doi.org/10.1038/nphys314)  
 578 [.1038/nphys314](https://doi.org/10.1038/nphys314) doi: 10.1038/nphys314
- 579 Popke, D., Stevens, B., & Voigt, A. (2013, January). Climate and climate change  
 580 in a radiative-convective equilibrium version of ECHAM6. *Journal of Advances*  
 581 *in Modeling Earth Systems*, 5(1), 1–14. Retrieved from [https://doi.org/10](https://doi.org/10.1029/2012ms000191)  
 582 [.1029/2012ms000191](https://doi.org/10.1029/2012ms000191) doi: 10.1029/2012ms000191
- 583 Posselt, D. J., van den Heever, S., Stephens, G., & Igel, M. R. (2012, January).  
 584 Changes in the interaction between tropical convection, radiation, and the  
 585 large-scale circulation in a warming environment. *Journal of Climate*, 25(2),  
 586 557–571. Retrieved from <https://doi.org/10.1175/2011jcli4167.1> doi:  
 587 [10.1175/2011jcli4167.1](https://doi.org/10.1175/2011jcli4167.1)
- 588 Posselt, D. J., van den Heever, S. C., & Stephens, G. L. (2008, April). Tri-  
 589 modal cloudiness and tropical stable layers in simulations of radiative con-  
 590 vective equilibrium. *Geophysical Research Letters*, 35(8). Retrieved from  
 591 <https://doi.org/10.1029/2007gl033029> doi: 10.1029/2007gl033029
- 592 Reid, J. S., Xian, P., Hyer, E. J., Flatau, M. K., Ramirez, E. M., Turk, F. J., ...  
 593 Maloney, E. D. (2012, February). Multi-scale meteorological conceptual  
 594 analysis of observed active fire hotspot activity and smoke optical depth in  
 595 the maritime continent. *Atmospheric Chemistry and Physics*, 12(4), 2117–  
 596 2147. Retrieved from <https://doi.org/10.5194/acp-12-2117-2012> doi:  
 597 [10.5194/acp-12-2117-2012](https://doi.org/10.5194/acp-12-2117-2012)

- 598 Rosenfeld, D., Lohmann, U., Raga, G. B., O'Dowd, C. D., Kulmala, M., Fuzzi,  
599 S., ... Andreae, M. O. (2008, September). Flood or drought: How do  
600 aerosols affect precipitation? *Science*, *321*(5894), 1309–1313. Retrieved from  
601 <https://doi.org/10.1126/science.1160606> doi: 10.1126/science.1160606
- 602 Salinas, S. V., Chew, B. N., Miettinen, J., Campbell, J. R., Welton, E. J., Reid,  
603 J. S., ... Liew, S. C. (2013, March). Physical and optical characteristics of  
604 the october 2010 haze event over singapore: A photometric and lidar analy-  
605 sis. *Atmospheric Research*, *122*, 555–570. Retrieved from [https://doi.org/](https://doi.org/10.1016/j.atmosres.2012.05.021)  
606 [10.1016/j.atmosres.2012.05.021](https://doi.org/10.1016/j.atmosres.2012.05.021) doi: 10.1016/j.atmosres.2012.05.021
- 607 Schiro, K. A., Neelin, J. D., Adams, D. K., & Lintner, B. R. (2016, September).  
608 Deep convection and column water vapor over tropical land versus tropical  
609 ocean: A comparison between the amazon and the tropical western pacific.  
610 *Journal of the Atmospheric Sciences*, *73*(10), 4043–4063. Retrieved from  
611 <https://doi.org/10.1175/jas-d-16-0119.1> doi: 10.1175/jas-d-16-0119.1
- 612 Seigel, R. B., van den Heever, S. C., & Saleeby, S. M. (2013, April). Mineral  
613 dust indirect effects and cloud radiative feedbacks of a simulated idealized  
614 nocturnal squall line. *Atmospheric Chemistry and Physics*, *13*(8), 4467–  
615 4485. Retrieved from <https://doi.org/10.5194/acp-13-4467-2013> doi:  
616 10.5194/acp-13-4467-2013
- 617 Shpund, J., Khain, A., & Rosenfeld, D. (2019, August). Effects of sea spray on mi-  
618 crophysics and intensity of deep convective clouds under strong winds. *Jour-  
619 nal of Geophysical Research: Atmospheres*, *124*(16), 9484–9509. Retrieved from  
620 <https://doi.org/10.1029/2018jd029893> doi: 10.1029/2018jd029893
- 621 Singh, M. S., & O'Gorman, P. A. (2013, August). Influence of entrainment  
622 on the thermal stratification in simulations of radiative-convective equilib-  
623 rium. *Geophysical Research Letters*, *40*(16), 4398–4403. Retrieved from  
624 <https://doi.org/10.1002/grl.50796> doi: 10.1002/grl.50796
- 625 Singh, M. S., & O'Gorman, P. A. (2015, June). Increases in moist-convective up-  
626 draught velocities with warming in radiative-convective equilibrium. *Quarterly  
627 Journal of the Royal Meteorological Society*, *141*(692), 2828–2838. Retrieved  
628 from <https://doi.org/10.1002/qj.2567> doi: 10.1002/qj.2567
- 629 Sobel, A. H., Nilsson, J., & Polvani, L. M. (2001, December). The weak temper-  
630 ature gradient approximation and balanced tropical moisture waves. *Journal  
631 of the Atmospheric Sciences*, *58*(23), 3650–3665. Retrieved from [https://doi  
632 .org/10.1175/1520-0469\(2001\)058<3650:twtgaa>2.0.co;2](https://doi.org/10.1175/1520-0469(2001)058<3650:twtgaa>2.0.co;2) doi: 10.1175/  
633 1520-0469(2001)058(3650:twtgaa)2.0.co;2
- 634 Stevens, B., Satoh, M., Auger, L., Biercamp, J., Bretherton, C. S., Chen, X., ...  
635 Zhou, L. (2019, September). DYAMOND: the DYnamics of the atmospheric  
636 general circulation modeled on non-hydrostatic domains. *Progress in Earth  
637 and Planetary Science*, *6*(1). Retrieved from [https://doi.org/10.1186/  
638 s40645-019-0304-z](https://doi.org/10.1186/s40645-019-0304-z) doi: 10.1186/s40645-019-0304-z
- 639 Storer, R. L., van den Heever, S. C., & L'Ecuyer, T. S. (2014, April). Observations  
640 of aerosol-induced convective invigoration in the tropical east atlantic. *Jour-  
641 nal of Geophysical Research: Atmospheres*, *119*(7), 3963–3975. Retrieved from  
642 <https://doi.org/10.1002/2013jd020272> doi: 10.1002/2013jd020272
- 643 Su, C.-Y., Chen, W.-T., Chen, J.-P., Chang, W.-Y., & Jou, B. J.-D. (2020). The  
644 impacts of cloud condensation nuclei on the extreme precipitation of a mon-  
645 soon coastal mesoscale convection system. *Terrestrial, Atmospheric and  
646 Oceanic Sciences*, *31*(2), 131–139. Retrieved from [https://doi.org/10.3319/  
647 tao.2019.11.29.01](https://doi.org/10.3319/tao.2019.11.29.01) doi: 10.3319/tao.2019.11.29.01
- 648 SU, C.-Y., CHEN, W.-T., WU, C.-M., & MA, H.-Y. (2022). Object-based eval-  
649 uation of tropical precipitation systems in DYAMOND simulations over the  
650 maritime continent. *Journal of the Meteorological Society of Japan. Ser. II*,  
651 *100*(4), 647–659. Retrieved from <https://doi.org/10.2151/jmsj.2022-033>  
652 doi: 10.2151/jmsj.2022-033

- 553 Su, C.-Y., Wu, C.-M., Chen, W.-T., & Chen, J.-H. (2021a, July). The effects of  
 554 the unified parameterization in the CWBGFS: the diurnal cycle of precip-  
 555 itation over land in the maritime continent. *Climate Dynamics*, *58*(1-2),  
 556 223–233. Retrieved from <https://doi.org/10.1007/s00382-021-05899-2>  
 557 doi: 10.1007/s00382-021-05899-2
- 558 Su, C.-Y., Wu, C.-M., Chen, W.-T., & Chen, J.-H. (2021b, October). Implementa-  
 559 tion of the unified representation of deep moist convection in the CWBGFS.  
 560 *Monthly Weather Review*, *149*(10), 3525–3539. Retrieved from [https://](https://doi.org/10.1175/mwr-d-21-0067.1)  
 561 [doi.org/10.1175/mwr-d-21-0067.1](https://doi.org/10.1175/mwr-d-21-0067.1) doi: 10.1175/mwr-d-21-0067.1
- 562 Tao, W.-K., Chen, J.-P., Li, Z., Wang, C., & Zhang, C. (2012, April). Impact  
 563 of aerosols on convective clouds and precipitation. *Reviews of Geophysics*,  
 564 *50*(2). Retrieved from <https://doi.org/10.1029/2011rg000369> doi:  
 565 10.1029/2011rg000369
- 566 Tao, W.-K., & Chern, J.-D. (2017, April). The impact of simulated mesoscale  
 567 convective systems on global precipitation: A multiscale modeling study. *Jour-  
 568 nal of Advances in Modeling Earth Systems*, *9*(2), 790–809. Retrieved from  
 569 <https://doi.org/10.1002/2016ms000836> doi: 10.1002/2016ms000836
- 570 Tao, W.-K., Li, X., Khain, A., Matsui, T., Lang, S., & Simpson, J. (2007, Decem-  
 571 ber). Role of atmospheric aerosol concentration on deep convective precipi-  
 572 tation: Cloud-resolving model simulations. *Journal of Geophysical Research*,  
 573 *112*(D24). Retrieved from <https://doi.org/10.1029/2007jd008728> doi:  
 574 10.1029/2007jd008728
- 575 Tompkins, A. M. (2001, March). Organization of tropical convection in low verti-  
 576 cal wind shears: The role of water vapor. *Journal of the Atmospheric Sciences*,  
 577 *58*(6), 529–545. Retrieved from [https://doi.org/10.1175/1520-0469\(2001\)](https://doi.org/10.1175/1520-0469(2001)058<0529:ootcil>2.0.co;2)  
 578 [058<0529:ootcil>2.0.co;2](https://doi.org/10.1175/1520-0469(2001)058(0529:ootcil)2.0.co;2) doi: 10.1175/1520-0469(2001)058(0529:ootcil)2.0  
 579 .co;2
- 580 Tsai, W.-M., & Wu, C.-M. (2017, September). The environment of aggregated  
 581 deep convection. *Journal of Advances in Modeling Earth Systems*, *9*(5), 2061–  
 582 2078. Retrieved from <https://doi.org/10.1002/2017ms000967> doi: 10  
 583 .1002/2017ms000967
- 584 van den Heever, S. C., & Cotton, W. R. (2007, June). Urban aerosol impacts on  
 585 downwind convective storms. *Journal of Applied Meteorology and Climatology*,  
 586 *46*(6), 828–850. Retrieved from <https://doi.org/10.1175/jam2492.1> doi:  
 587 10.1175/jam2492.1
- 588 van den Heever, S. C., Stephens, G. L., & Wood, N. B. (2011, April). Aerosol  
 589 indirect effects on tropical convection characteristics under conditions of ra-  
 590 diative–convective equilibrium. *Journal of the Atmospheric Sciences*, *68*(4),  
 591 699–718. Retrieved from <https://doi.org/10.1175/2010jas3603.1> doi:  
 592 10.1175/2010jas3603.1
- 593 Varble, A. (2018, April). Erroneous attribution of deep convective invigoration to  
 594 aerosol concentration. *Journal of the Atmospheric Sciences*, *75*(4), 1351–1368.  
 595 Retrieved from <https://doi.org/10.1175/jas-d-17-0217.1> doi: 10.1175/  
 596 jas-d-17-0217.1
- 597 Wing, A. A., Emanuel, K., Holloway, C. E., & Muller, C. (2017, February). Con-  
 598 vective self-aggregation in numerical simulations: A review. *Surveys in Geo-  
 599 physics*, *38*(6), 1173–1197. Retrieved from [https://doi.org/10.1007/s10712-](https://doi.org/10.1007/s10712-017-9408-4)  
 600 [017-9408-4](https://doi.org/10.1007/s10712-017-9408-4) doi: 10.1007/s10712-017-9408-4
- 601 Wing, A. A., & Emanuel, K. A. (2014, February). Physical mechanisms controlling  
 602 self-aggregation of convection in idealized numerical modeling simulations.  
 603 *Journal of Advances in Modeling Earth Systems*, *6*(1), 59–74. Retrieved from  
 604 <https://doi.org/10.1002/2013ms000269> doi: 10.1002/2013ms000269
- 605 Wing, A. A., Reed, K. A., Satoh, M., Stevens, B., Bony, S., & Ohno, T. (2018,  
 606 March). Radiative–convective equilibrium model intercomparison project.  
 607 *Geoscientific Model Development*, *11*(2), 793–813. Retrieved from [https://](https://doi.org/10.5194/gmd-11-793-2018)

- 708 doi.org/10.5194/gmd-11-793-2018 doi: 10.5194/gmd-11-793-2018  
709 Wing, A. A., Stauffer, C. L., Becker, T., Reed, K. A., Ahn, M.-S., Arnold, N. P.,  
710 ... Zhao, M. (2020, September). Clouds and convective self-aggregation  
711 in a multimodel ensemble of radiative-convective equilibrium simulations.  
712 *Journal of Advances in Modeling Earth Systems*, 12(9). Retrieved from  
713 <https://doi.org/10.1029/2020ms002138> doi: 10.1029/2020ms002138  
714 Wu, C.-M., & Arakawa, A. (2014, May). A unified representation of deep moist con-  
715 vection in numerical modeling of the atmosphere. part II. *Journal of the At-*  
716 *mospheric Sciences*, 71(6), 2089–2103. Retrieved from [https://doi.org/10](https://doi.org/10.1175/jas-d-13-0382.1)  
717 [.1175/jas-d-13-0382.1](https://doi.org/10.1175/jas-d-13-0382.1) doi: 10.1175/jas-d-13-0382.1  
718 Yanase, T., Nishizawa, S., Miura, H., & Tomita, H. (2022, September). Character-  
719 istic form and distance in high-level hierarchical structure of self-aggregated  
720 clouds in radiative-convective equilibrium. *Geophysical Research Letters*,  
721 49(18). Retrieved from <https://doi.org/10.1029/2022gl1100000> doi:  
722 10.1029/2022gl1100000  
723 Yuan, J., & Houze, R. A. (2010, November). Global variability of mesoscale con-  
724 vective system anvil structure from a-train satellite data. *Journal of Climate*,  
725 23(21), 5864–5888. Retrieved from [https://doi.org/10.1175/2010jcli3671](https://doi.org/10.1175/2010jcli3671.1)  
726 [.1](https://doi.org/10.1175/2010jcli3671.1) doi: 10.1175/2010jcli3671.1  
727 Zhang, C. (2013, December). Madden–julian oscillation: Bridging weather and cli-  
728 mate. *Bulletin of the American Meteorological Society*, 94(12), 1849–1870. Re-  
729 trieved from <https://doi.org/10.1175/bams-d-12-00026.1> doi: 10.1175/  
730 [bams-d-12-00026.1](https://doi.org/10.1175/bams-d-12-00026.1)  
731 Zhang, C., & Ling, J. (2017, May). Barrier effect of the indo-pacific maritime con-  
732 tinent on the MJO: Perspectives from tracking MJO precipitation. *Journal of*  
733 *Climate*, 30(9), 3439–3459. Retrieved from [https://doi.org/10.1175/jcli](https://doi.org/10.1175/jcli-d-16-0614.1)  
734 [-d-16-0614.1](https://doi.org/10.1175/jcli-d-16-0614.1) doi: 10.1175/jcli-d-16-0614.1

Figure 1.

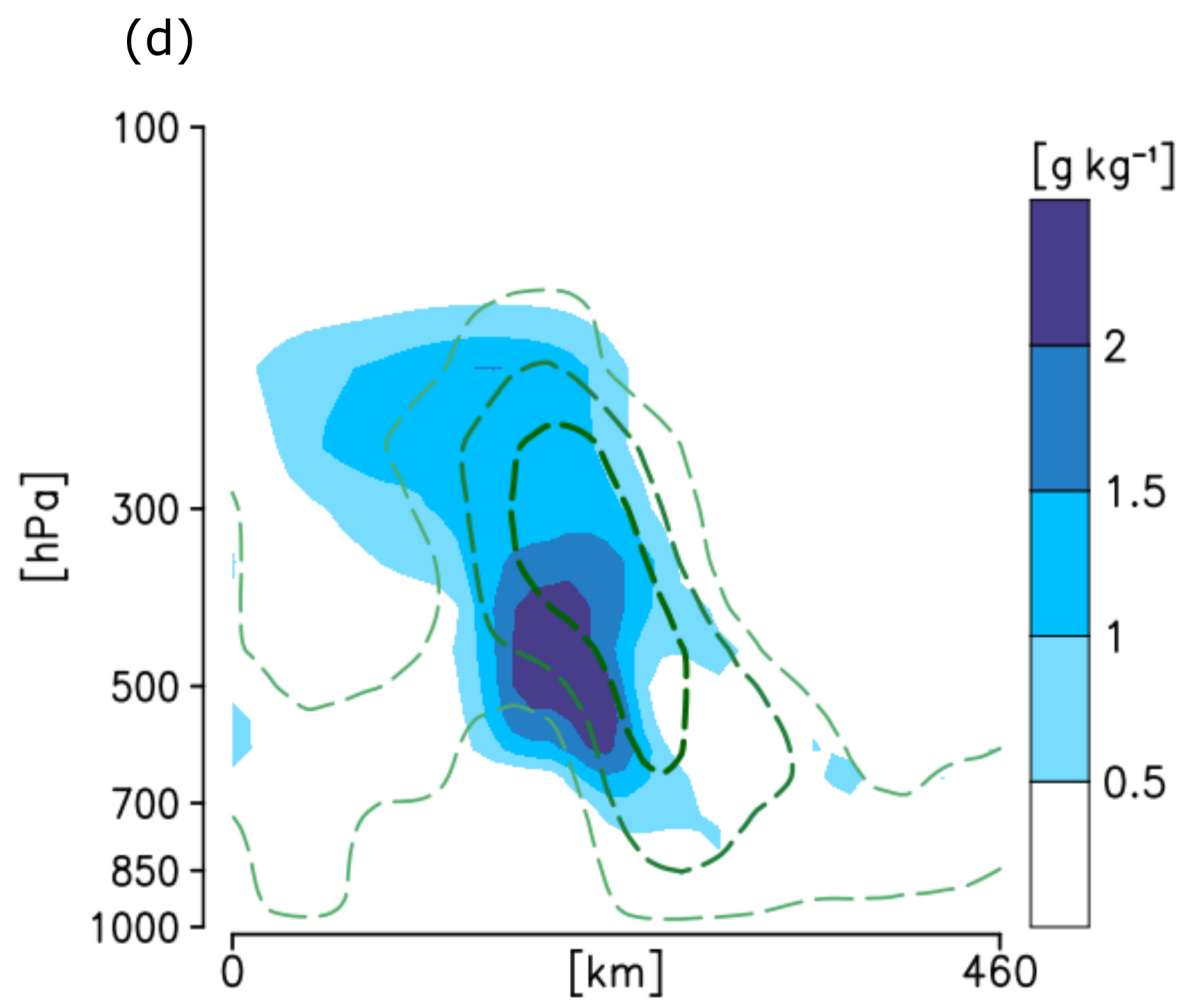
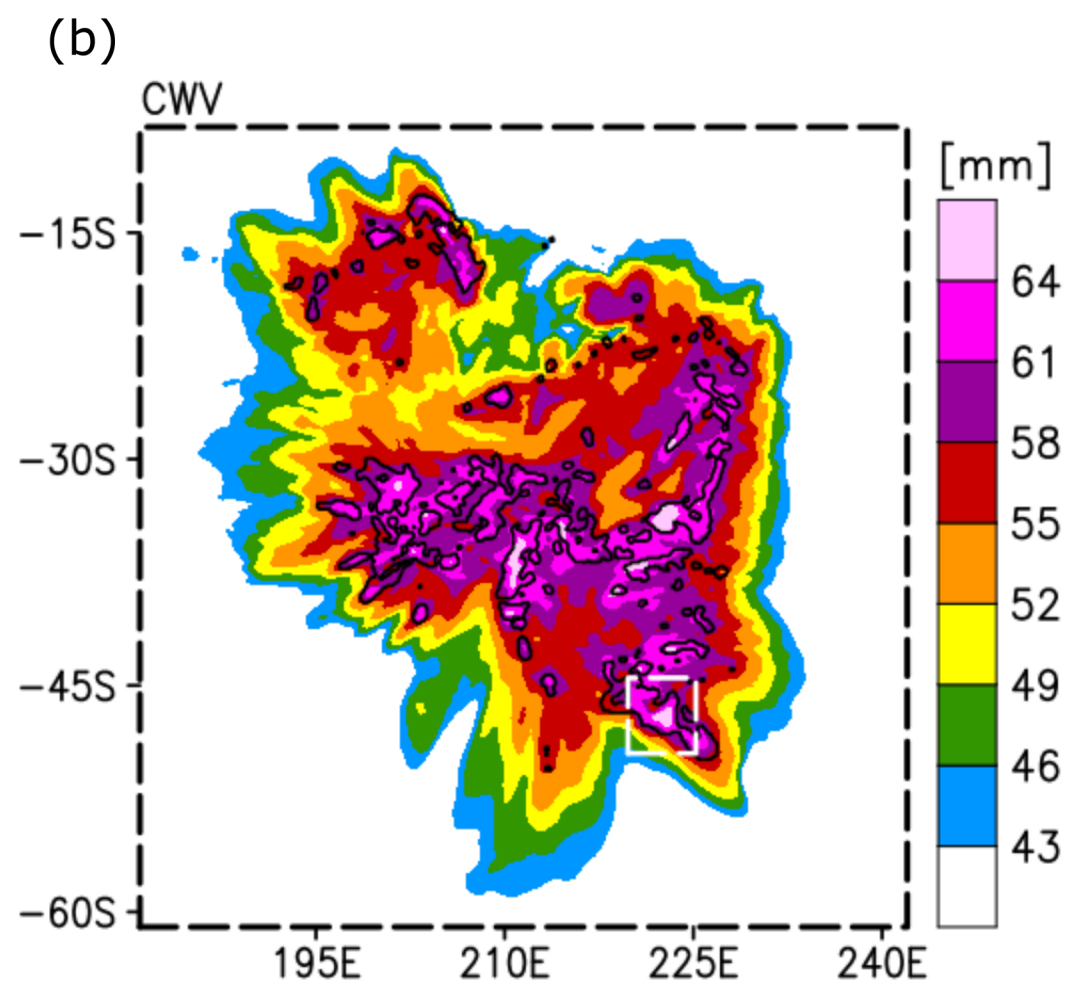
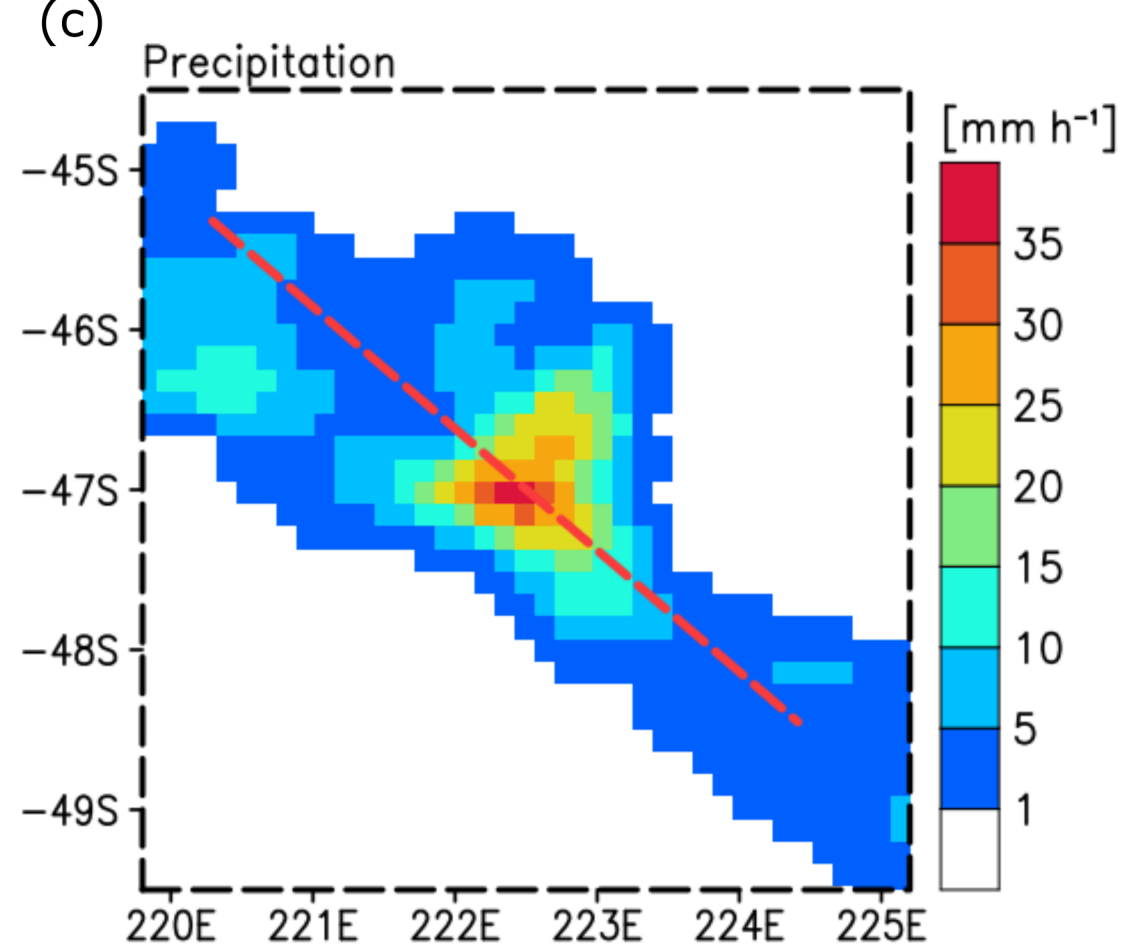
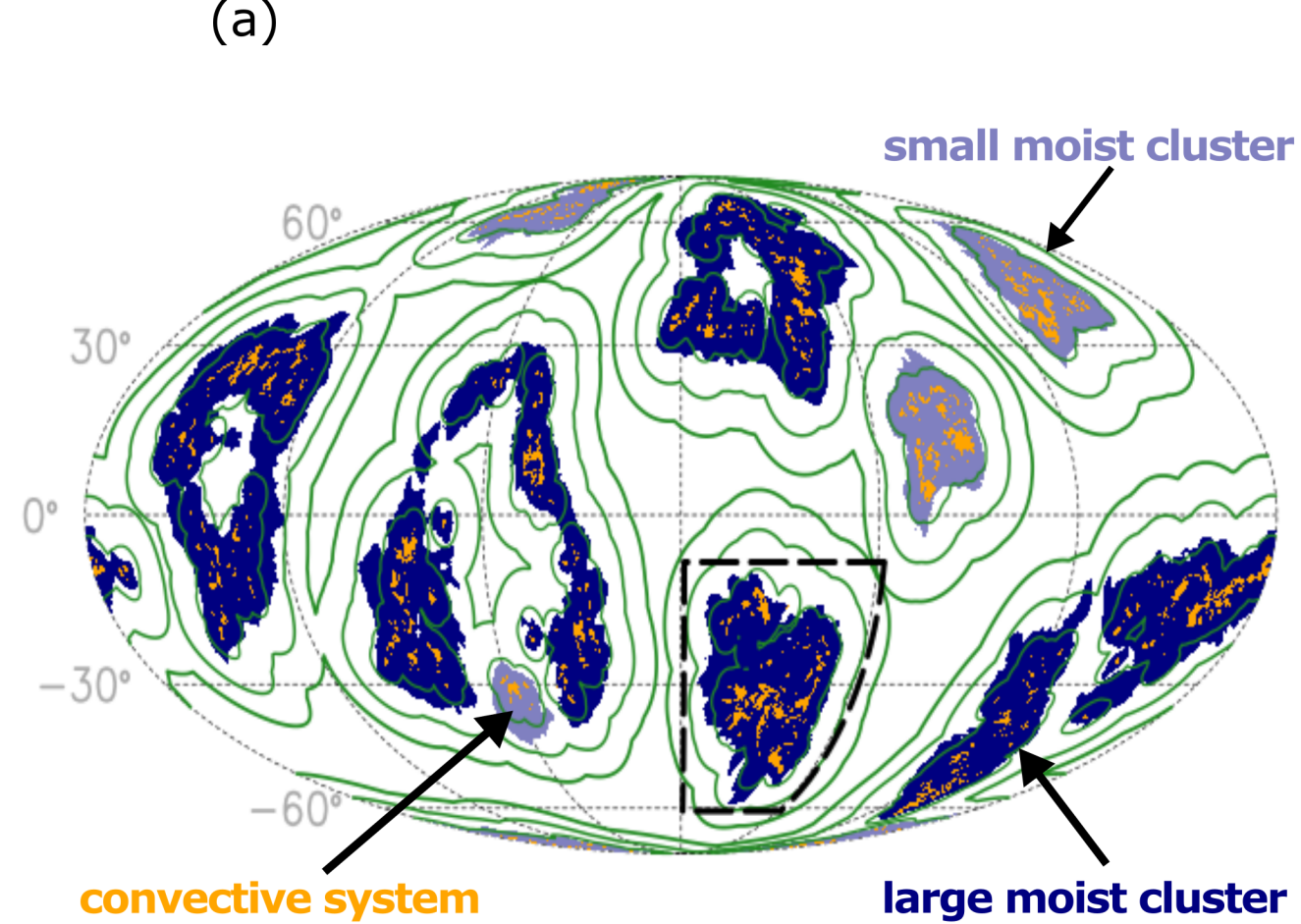


Figure 2.

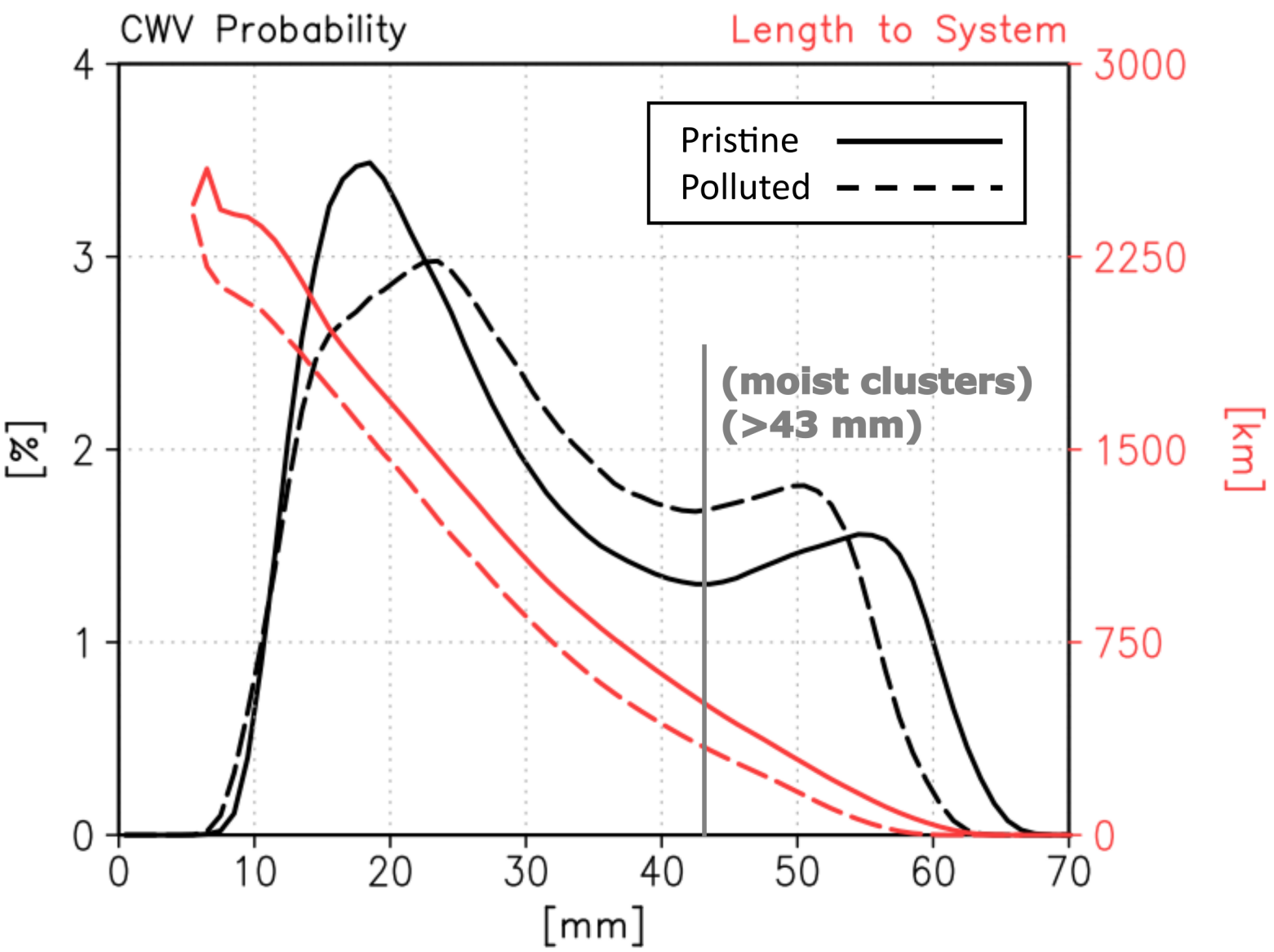


Figure 3.

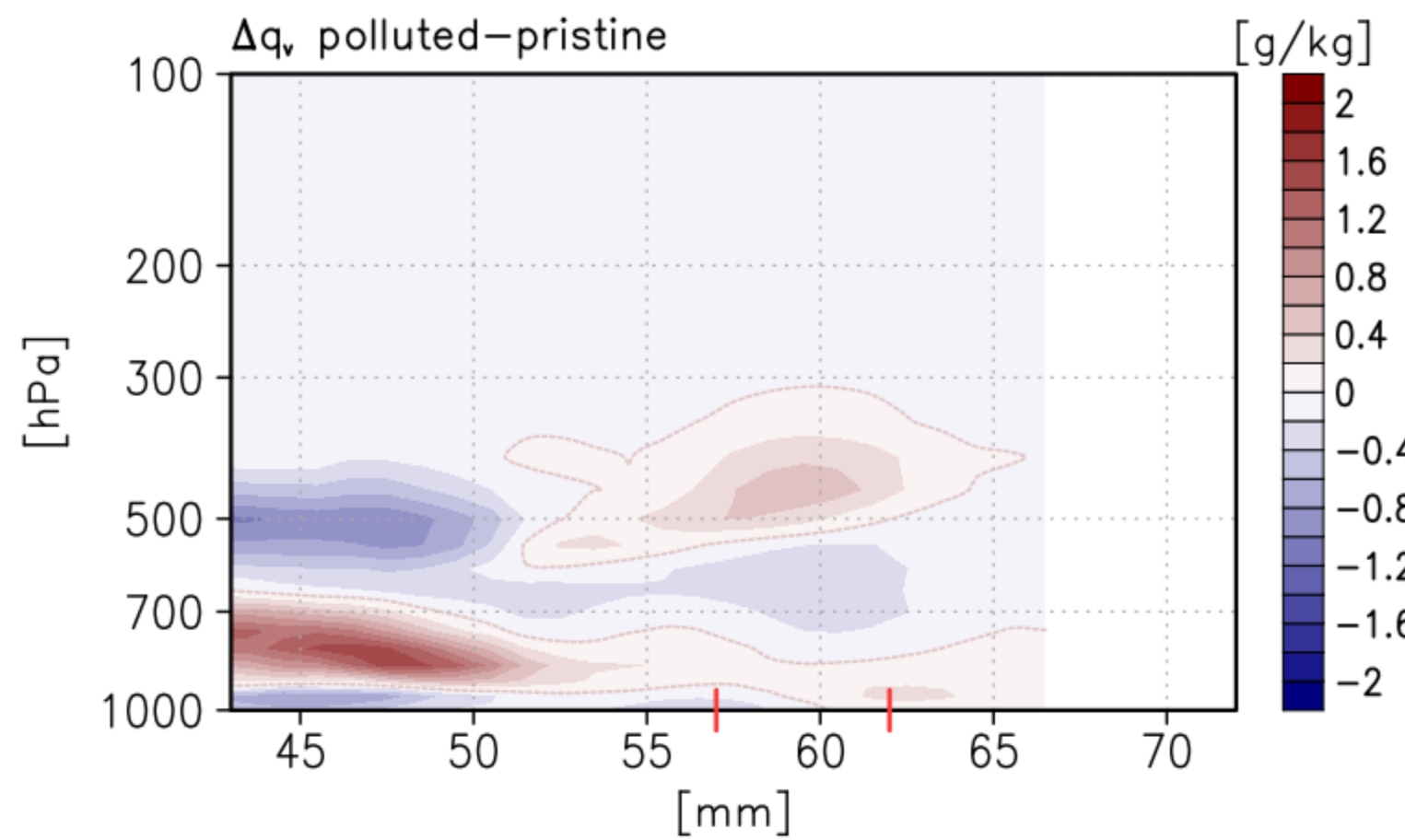
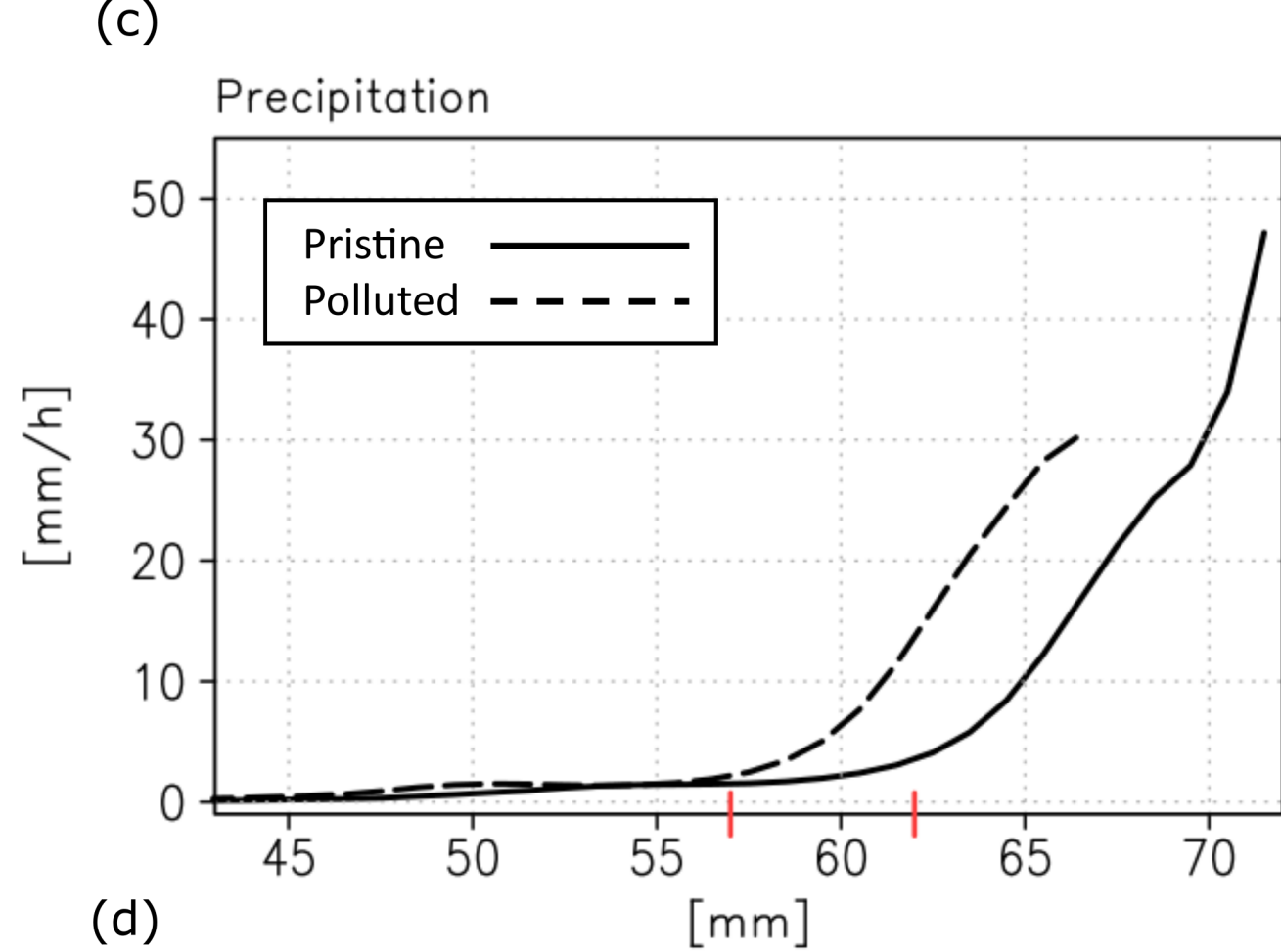
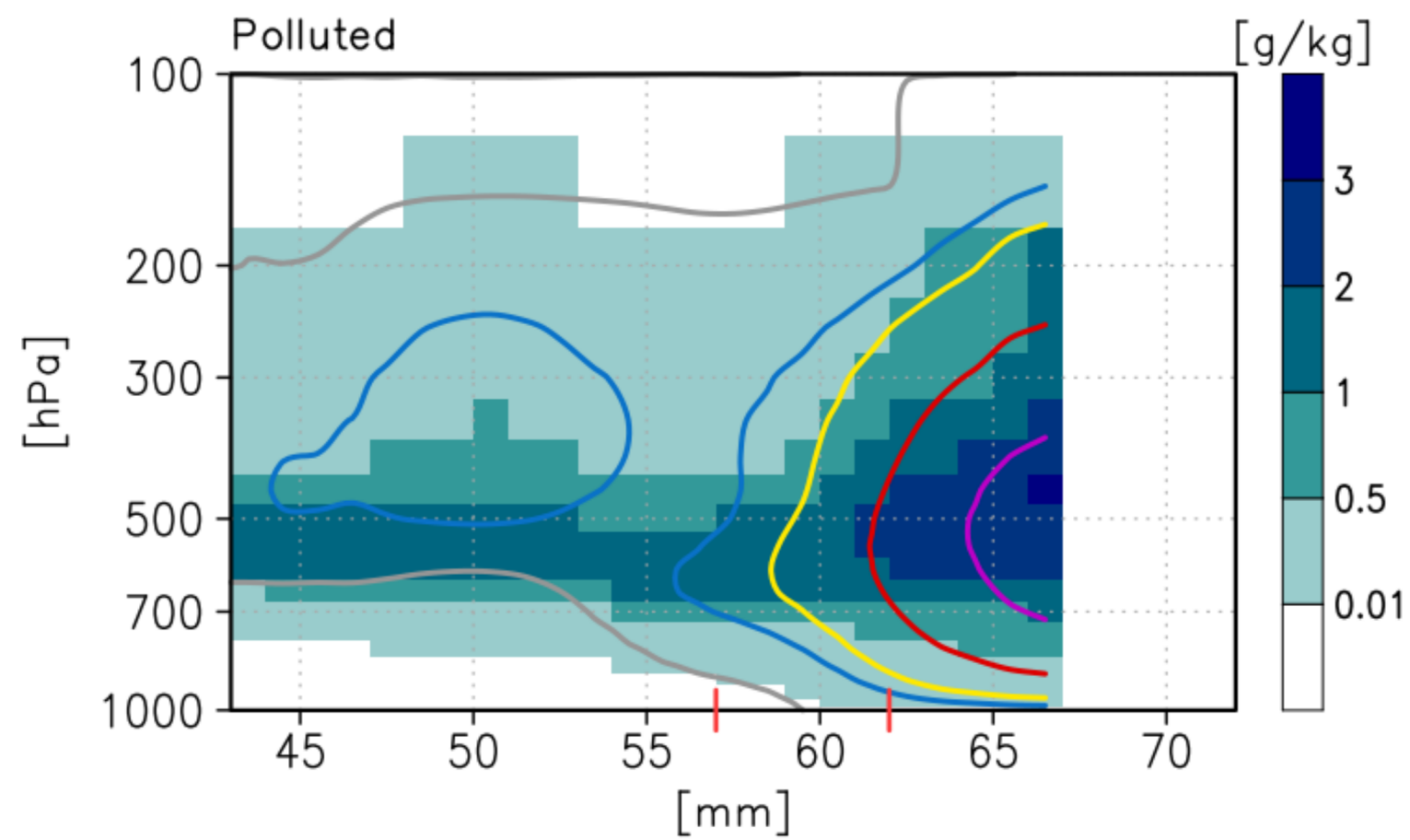
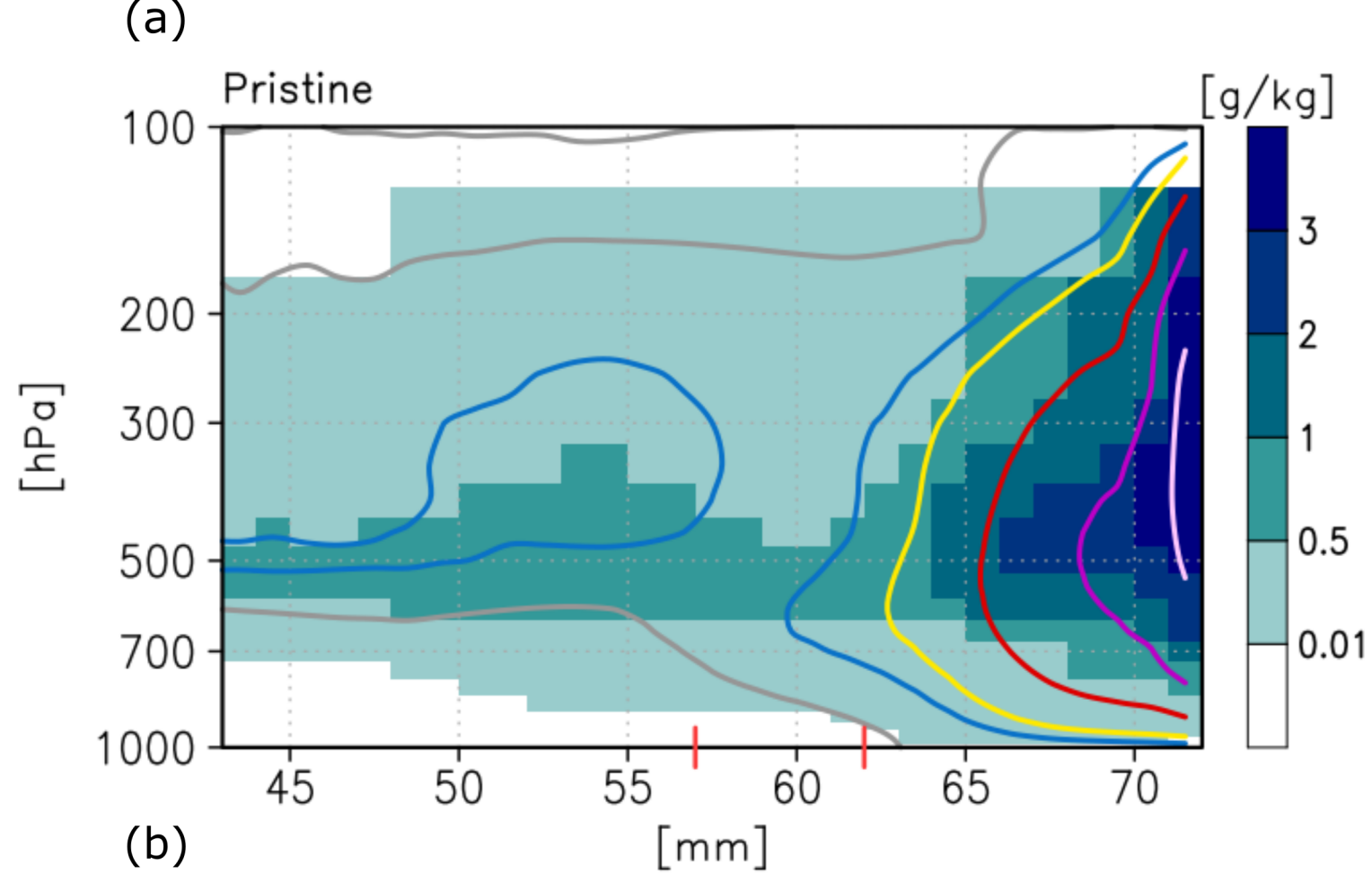
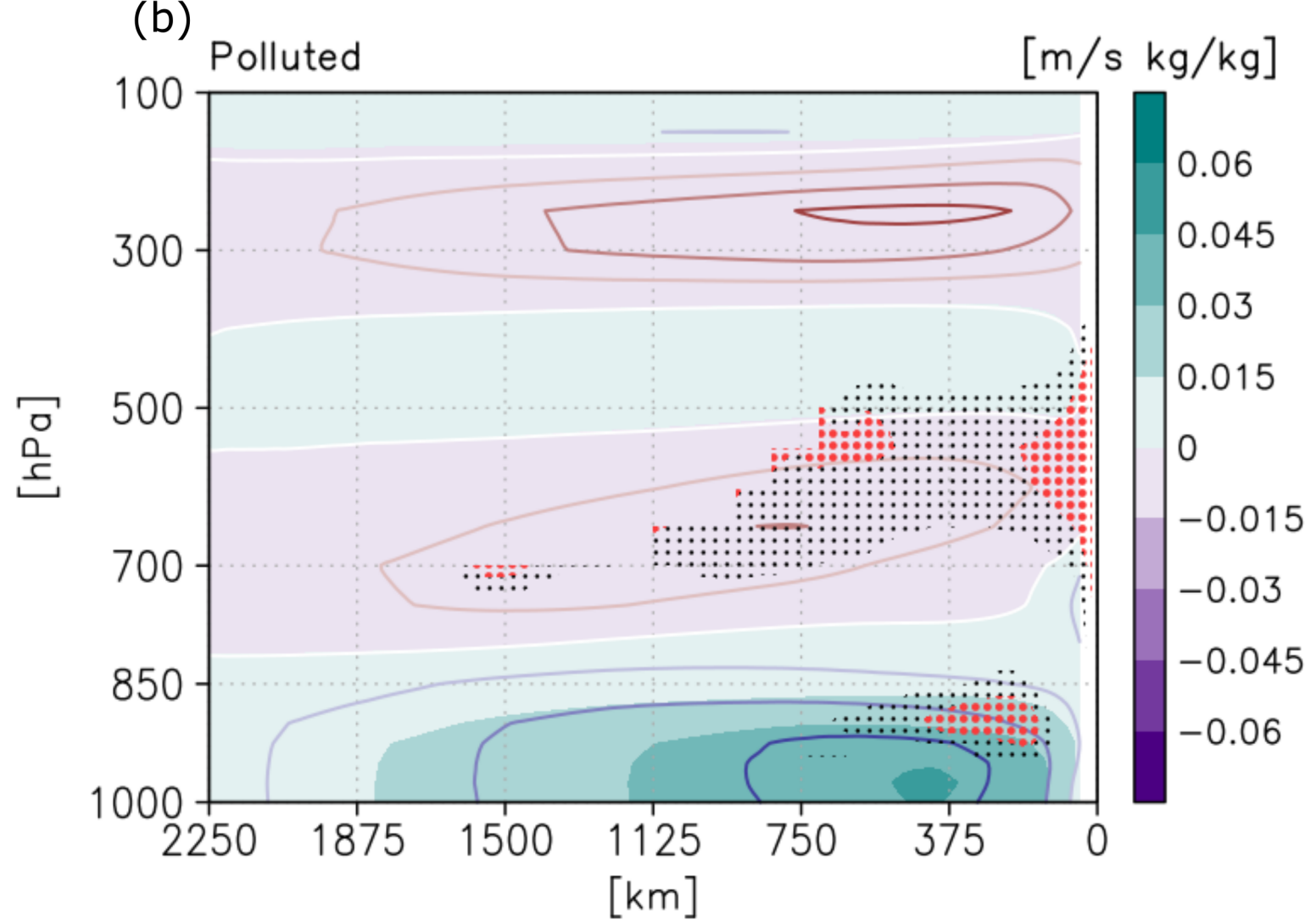
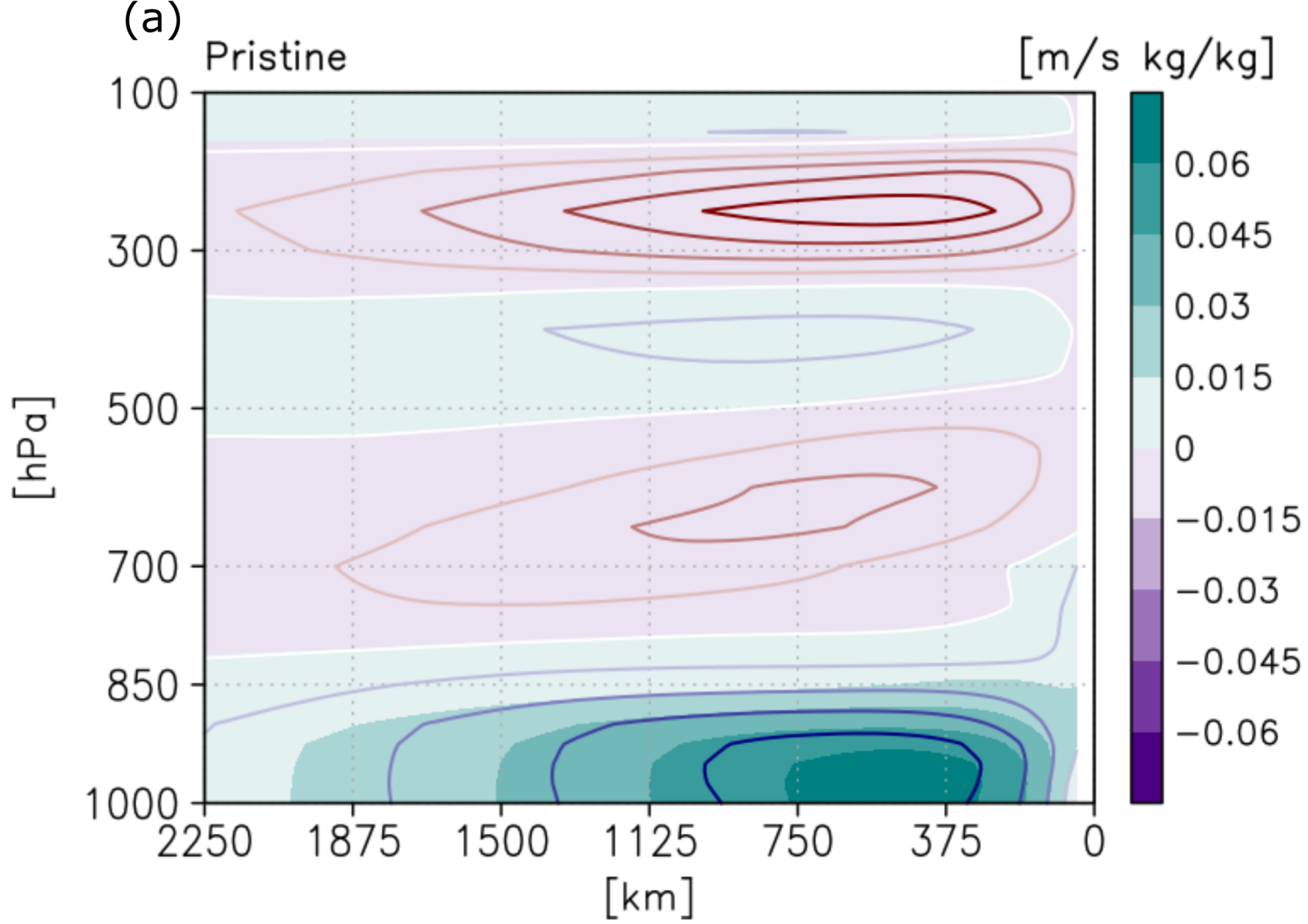


Figure 4.



1                   **Modulation of Tropical Convection-circulation**  
2                   **Interaction by Aerosol Indirect Effects in a Global**  
3                   **Convection-permitting Model**

4                   **Chun-Yian Su<sup>1,2</sup>, Chien-Ming Wu<sup>2</sup>, Wei-Ting Chen<sup>2</sup>, and John M. Peters<sup>1</sup>**

5                   <sup>1</sup>Department of Meteorology and Atmospheric Science, The Pennsylvania State University, University  
6                   Park, PA

7                   <sup>2</sup>Department of Atmospheric Sciences, National Taiwan University, Taipei city, Taiwan

8                   **Key Points:**

- 9                   • Simulations of the global convection-permitting model provide a new perspective  
10                  on aerosol indirect effects.  
11                  • Pollution facilitates the development of deep convection in a drier environment.  
12                  • The response of large-scale circulation to pollution limits the intensity of maxi-  
13                  mum precipitation.

---

Corresponding author: Chien-Ming Wu, [mog@as.ntu.edu.tw](mailto:mog@as.ntu.edu.tw)

**Abstract**

Observations suggest tropical convection intensifies when aerosol concentrations enhance, but quantitative estimations of this effect remain highly uncertain. Leading theories for explaining the intensification are based on the dynamical response of convection to changes in cloud microphysics independently from possible changes in the environment. Here, we provide a new perspective on aerosol indirect effects on tropical convection by using a global convection-permitting model that realistically simulates convection-circulation interaction. Simulations of radiative-convective equilibrium show that pollution facilitates the development of deep convection in a drier environment, but cloud condensates are more likely to be exported from moist clusters to dry areas, impeding the large-scale moisture-convection feedback and limiting the intensity of maximum precipitation (30 vs. 47 mm h<sup>-1</sup>). Our results emphasize the importance of allowing atmospheric phenomena to evolve continuously across spatial and temporal scales in simulations when investigating the response of tropical convection to changes in cloud microphysics.

**Plain Language Summary**

How does air pollution affect thunderstorm intensity over the tropical ocean? Past studies have proposed different opinions but generally neglect the interplay between the development of thunderstorms and the long-range movement of air that redistributes the Earth's thermal energy and moisture. Here, we address this question by investigating results from numerical experiments in which the global domain is used to simulate the response of individual thunderstorms and large-scale air motion to pollution. Our results show that tropical thunderstorms with given moisture are more vigorous under the polluted scenario. However, pollution makes the thunderstorms keep less moisture in their surroundings, limiting the maximum intensity of thunderstorms and weakening the large-scale air motion that supplies moisture to thunderstorms. Our results suggest that the interplay between the development of thunderstorms and the long-range movement of air is crucial in determining the effects of pollution in the tropical atmosphere.

**1 Introduction**

Deep convective clouds (DCCs) play a critical role in the global climate system via their role in the Earth's energy budget (Arakawa, 2004; Hartmann et al., 2001). They can aggregate into organized convective systems that span hundreds to a thousand kilometers (Houze, 2004) and contribute significantly to tropical rainfall (Chen et al., 2021; Houze et al., 2015; Nesbitt et al., 2006; Tao & Chern, 2017; Yuan & Houze, 2010). Observations suggest that updrafts of tropical DCCs can be invigorated by enhanced aerosol concentrations that arise from human activities and natural sources (Andreae et al., 2004; Koren et al., 2008; Niu & Li, 2012; Pan et al., 2021; Storer et al., 2014). By acting as cloud condensate nuclei (CCN) or ice nuclei (IN), aerosols change cloud properties by influencing cloud microphysics and dynamics, meanwhile influencing cloud-radiation feedbacks (i.e., aerosol indirect effects (AIEs); see reviews of Fan et al. (2016) and Tao et al. (2012)). A deeper understanding of AIEs on tropical DCCs and organized convective systems could improve the prediction of extreme precipitation events in global weather and climate models. However, the underlying mechanisms of how the updrafts are invigorated remain elusive and are often debated (Fan et al., 2018; Fan & Khain, 2021; W. W. Grabowski & Morrison, 2020, 2021; Igel & van den Heever, 2021). A particular challenge of understanding AIEs using observations is that the observed aerosol concentrations in the environments of DCCs often covary with other meteorological factors, such as convective available potential energy and vertical wind shear (W. W. Grabowski, 2018; Nishant & Sherwood, 2017; Varble, 2018), and the influences of meteorological and aerosol variability are difficult to disentangle from one another. Further, there is evidence from simulations that AIEs on DCCs vary as a function of meteorological conditions such as shear

64 and humidity (Fan et al., 2009; van den Heever & Cotton, 2007; Khain et al., 2008; Ko-  
65 ren et al., 2010; Z. Lebo, 2018), which further complicates our ability to isolate the aerosol  
66 effects from other meteorological processes. AIEs are underrepresented in global climate  
67 models because of these knowledge gaps, which contributes to considerable uncertainty  
68 in estimating human climate forcing (Forster et al., 2021).

69 To investigate the aerosol indirect effects on DCCs that interact with their surround-  
70 ing environment, Abbott and Cronin (2021) carried out simulations using a small do-  
71 main ( $128 \times 128 \text{ km}^2$ ) three-dimension cloud-resolving model (3-D CRM) with parame-  
72 terized large-scale dynamics under the weak temperature gradient (WTG) approxima-  
73 tion (Sobel et al., 2001). Abbott and Cronin (2021) suggested that enhanced CCN con-  
74 centrations produce clouds that mix more condensed water into the surrounding air. This  
75 enhances the environment favorably for subsequent convection by moistening the free  
76 troposphere and reducing the deleterious effects of entrainment. The humidity-entrainment  
77 mechanism they proposed is distinct from past work, which linked stronger updrafts with  
78 latent heat released by cloud condensation (Fan et al., 2018) or freezing (Rosenfeld et  
79 al., 2008) independently from possible changes in the environment. Anber et al. (2019)  
80 also used a small domain ( $192 \times 192 \text{ km}^2$ ) 3-D CRM with parameterized large-scale dy-  
81 namics to carry out simulations with different number concentrations of CCN but found  
82 a contrasting result. In their simulations, convection and mean precipitation get weaker  
83 when the CCN concentration increases. They suggested that the changes are associated  
84 with the modulation of coupling between convective processes and large-scale motions  
85 that overall reduces surface enthalpy fluxes.

86 Using a large domain ( $10000 \text{ km}$ ) two-dimension CRM configured in radiative-convective  
87 equilibrium (RCE; Manabe & Strickler, 1964), van den Heever et al. (2011) found a weak  
88 response of the large-scale organization of convection and the domain-averaged precip-  
89 itation to enhanced CCN concentrations. They suggested that AIEs on the three trop-  
90 ical cloud modes are opposite in sign, offsetting each other, thus producing a weak domain-  
91 wide response. In contrast, a more recent study by Beydoun and Hoose (2019) that used  
92 a large channel-shaped domain ( $2000 \times 120 \text{ km}^2$ ) 3-D CRM found a comparatively large  
93 decrease in domain-averaged precipitation in their RCE simulations with enhanced CCN  
94 concentrations. They suggested that enhanced CCN concentrations lead to the weak-  
95 ened large-scale organization of convection, increased midlevel and upper-level clouds,  
96 decreased radiative cooling, and decreased domain-averaged precipitation.

97 The difference in the above findings is likely influenced by the representation of large-  
98 scale dynamics and the geometry of the simulation domain, which could modulate convection-  
99 circulation interaction hence affect the overall AIEs. For example, a horizontal scale of  
100 the model domain larger than  $5000 \text{ km}$  was suggested to be large enough to represent  
101 the natural scale of large-scale organization of convection (Matsugishi & Satoh, 2022;  
102 Patrizio & Randall, 2019; Yanase et al., 2022). Advances in computational resources have  
103 allowed for global model simulations that explicitly simulate deep convection (Stevens  
104 et al., 2019). These global convection-permitting models have been applied to investi-  
105 gate how clouds and convective processes couple to large-scale circulation and determine  
106 cloud feedbacks and climate sensitivity (Wing et al., 2020). However, how is the coupling  
107 of DCCs and large-scale circulations affected by enhanced aerosol concentrations has not  
108 been fully understood.

109 This study aims to investigate the modulation of tropical convection-circulation in-  
110 teraction by AIEs in global simulations that simultaneously resolve the dynamical re-  
111 sponse of convection to changes in cloud microphysics and allow large-scale circulations  
112 to naturally develop since the horizontal scale is not artificially constrained by the do-  
113 main size or shape. The modulation of tropical convection-circulation interaction by AIEs  
114 is demonstrated by analyzing the responses of moisture distribution, convection struc-  
115 tures, and large-scale circulation to pollution. Section 2 introduces more details about

116 the model and the experiment design. Section 3 describes the results, and the summary  
 117 and discussion are presented in section 4.

## 118 2 Model Description and Experiment Design

119 We use the Central Weather Bureau Global Forecast System (CWBGFS; Su et al.,  
 120 2021a, 2021b; SU et al., 2022), which is a global convection-permitting model run at the  
 121 horizontal resolution of 15 km, to carry out our experiments. Deep convection in the CW-  
 122 BGFS is represented by the unified relaxed Arakawa-Schubert scheme (URAS; Su et al.,  
 123 2021b) in which the representation transitions from the parameterization to the explicit  
 124 simulation as the diagnosed convective updraft fraction increases (Arakawa & Wu, 2013;  
 125 Wu & Arakawa, 2014). Hence, the CWBGFS with the URAS can explicitly but efficiently  
 126 simulate deep convection and convection-circulation interaction on the global scale. This  
 127 model partially resolve circulations in organized convective systems and reproduce the  
 128 observed feature of convective systems that stronger extreme precipitation occurs in hor-  
 129 izontally larger systems (Hamada et al., 2014; SU et al., 2022).

130 The CWBGFS uses the two-moment Predicted Particle Properties bulk microphysics  
 131 scheme (P3; Morrison & Milbrandt, 2015) to represent cloud microphysical processes,  
 132 including cloud-aerosol interaction. The aerosol concentration prescribed in P3 is fixed  
 133 throughout the integration and acts as CCN. Cloud-aerosol interaction is not included  
 134 in the URAS. In our simulations, the averaged percentage of precipitation produced by  
 135 explicitly simulated convection is more than 93 % over precipitation events stronger than  
 136 5 mm h<sup>-1</sup>, indicating that most of the cloud-aerosol interactions associated with deep con-  
 137 vection are resolved. The rest of the descriptions regarding physics suites and the dy-  
 138 namic core of the CWBGFS can be found in Su et al. (2021a).

139 Two idealized non-rotating aqua-planet simulations configured in RCE are carried  
 140 out. Simulations in RCE have been extensively used to investigate feedback among clouds,  
 141 environmental moisture, radiation, and precipitation (Bretherton et al., 2005; Coppin  
 142 & Bony, 2015; Cronin & Wing, 2017; Emanuel et al., 2014; Holloway & Woolnough, 2016;  
 143 Pendergrass et al., 2016; Popke et al., 2013; Singh & O’Gorman, 2013, 2015; Wing & Emanuel,  
 144 2014; Wing et al., 2020), and therefore provide an ideal experimental setting to study  
 145 AIEs. Under certain circumstances, convection in RCE spontaneously self-organizes into  
 146 one or more moist ascending clusters surrounded by dry subsiding convection-free ar-  
 147 eas in simulations configured in non-rotating RCE (convective self-aggregation (CSA);  
 148 C. Muller et al., 2022; Wing et al., 2017). We note that CSA occurs in the simulations  
 149 of van den Heever et al. (2011) and Beydoun and Hoose (2019).

150 The simulations are initialized with an analytic sounding (Wing et al., 2018) that  
 151 approximates the moist tropical sounding of Dunion (2011), and the initial horizontal  
 152 winds are set to zero. The initial surface pressure of all grid columns is 1014.8 hPa. The  
 153 incoming solar radiation (409.6 W m<sup>-2</sup>), the sea surface temperature (300 K), and the  
 154 surface albedo (0.07) are spatially uniform and constant in time. The simulations are  
 155 run for 120 days, and the random perturbation of temperature from 0.1 to 0.02 K is added  
 156 to the five lowest model levels in the first 20 days to speed up convection initiation. The  
 157 only difference between the two simulations is the prescribed spatially uniform aerosol  
 158 number mixing ratio set in P3. They are set at  $3 \times 10^8$  kg<sup>-1</sup> and  $3 \times 10^{10}$  kg<sup>-1</sup>, represent-  
 159 ing the pristine and polluted scenarios, respectively. The scenarios here are referred to  
 160 the marine environment (Andreae, 2009) and the urban environment (Chang et al., 2021)  
 161 and are used to evaluate the upper bound of AIEs on convection-circulation interaction.  
 162 In the following section, 30 days of hourly output (days 90 to 120) are analyzed when  
 163 the simulation is in an RCE state.

164 The overall results of the pristine run are showcased in Fig. 1, demonstrating that  
 165 our simulations resemble the global model simulations in the RCE model intercompar-

166 ison project (Wing et al., 2018, 2020), in which convection self-organizing into multiple  
 167 moist clusters (Fig. 1a). Fig. 1b shows the spatial distribution of column water vapor  
 168 (CWV) of a moist cluster, indicating high heterogeneity that is coupled to spatial convec-  
 169 tion structures. Precipitation stronger than  $30 \text{ mm h}^{-1}$  (Fig. 1c) is found in a convec-  
 170 tive system with intense resolved updrafts ( $>1 \text{ m s}^{-1}$ ) (Fig. 1d). Fig. 1 with more detail  
 171 will be introduced in the following section.

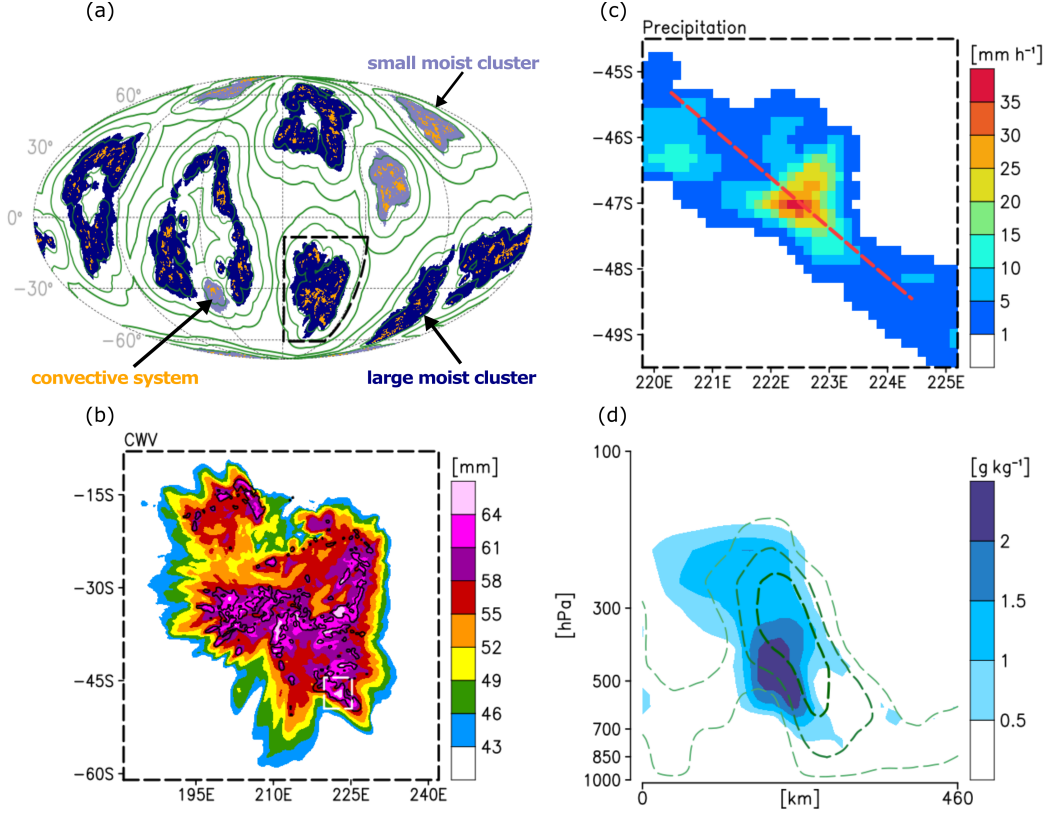


**Figure 1.** A snapshot of moist clusters smaller (light blue shaded) and larger (navy shaded) than 1000 km of horizontal scale, convective systems (orange shaded), and distance to the nearest convective system (green contours of 375, 1125, 1875 km) of the pristine run on day 106.5 (a). Column water vapor (mm) and convective systems (black contours) in a moist cluster (b), which the domain is demonstrated by the black dashed lines in (a). Precipitation intensity ( $\text{mm h}^{-1}$ ) of a convective system (c), which the domain is demonstrated by the white dashed lines in (b). The vertical profiles of mixed-phase cloud condensates (shaded) and vertical velocity (green contours of 0.1, 0.5,  $1 \text{ m s}^{-1}$ ) (d) along the red dashed line in (c). See the context for the definition of moist clusters and convective systems. The horizontal scale is determined by the square root of the cluster’s horizontal area.

### 3 Results

We start from demonstrating the response of moisture probability distribution to enhanced CCN concentrations. In both runs, the distribution of CWV is bimodal (Fig. 2). The bimodality suggests the presence of an aggregated state (Arnold & Randall, 2015; Tsai & Wu, 2017) which is maintained by large-scale circulation. The difference between the two local maxima of the bimodality is smaller in the polluted run, suggesting AIEs

178 drive columns away from both moist and dry equilibria in the pristine run. We use the  
 179 CWV value that corresponds to the smallest value along the curve in Fig. 2 between the  
 180 local maxima at dry and moist CWV values as the threshold to define moist clusters (i.e.,  
 181 43 mm in both runs). The difference in area coverage percentage of moist clusters in the  
 182 global domain between the two runs is less than 3 %. The moist clusters in the polluted  
 183 run are notably drier than that in the pristine run. Further, the number of moist clusters  
 184 in the polluted run is 23 % more than that in the pristine run. Sixty-five percent  
 185 of moist clusters are smaller than 1000 km of horizontal scale in the polluted run, and  
 186 there are 45 % of them in the pristine run.

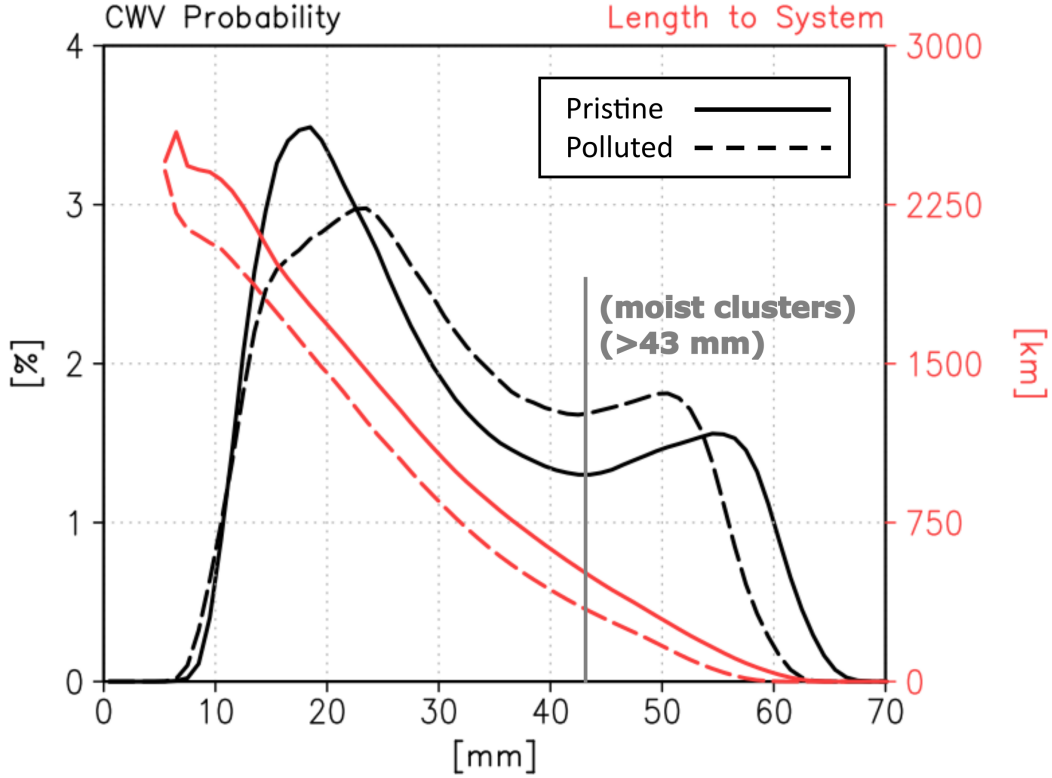


**Figure 2.** Probability distribution of column water vapor (black) and distance to the nearest convective system conditional sampled by column water vapor (red) from days 90 to 120. The gray line labels 43 mm of column water vapor, which is set as the criteria for defining a moist cluster.

187 We evaluate AIEs by first identifying the updraft regions of convective systems as  
 188 laterally connected columns of vertical velocity  $>0.1 \text{ m s}^{-1}$  in any level between 700 to  
 189 400 hPa (Fig. 1a-b). A critical characteristic of tropical deep moist convection is the rapid  
 190 intensification of precipitation once CWV has exceeded a critical value, which character-  
 191 izes the effect of water vapor on the buoyancy of clouds through entrainment (Bretherton  
 192 et al., 2004; Neelin et al., 2009; Peters & Neelin, 2006). Hence, we investigate the influ-  
 193 ence of pollution on this precipitation-CWV dependency. Analyses among all updraft  
 194 regions with a given CWV indicate that both of our simulations mimic the precipitation-  
 195 CWV dependency seen in nature, with a rapid increase in mixed-phase cloud condensate,  
 196 updraft intensity (Fig. 3a-b), and precipitation (Fig. 3c) occurring in both simu-  
 197 lations above a certain threshold in CWV. However, a distinct difference of the polluted  
 198 run from the pristine one is that the threshold CWV which heralds the increase in con-

199 vective intensity occurs at a lower CWV value (57 mm) than it does in the pristine run  
200 (62 mm).

201 Fig. 3a-b show that the vertical profiles to the right of the CWV thresholds resem-  
202 ble the convection structures of deep convection at the developing and mature stage, and  
203 the profiles to the left resemble deep convection at the dissipating stage, in which mixed-  
204 phase cloud condensates concentrate at mid-level free atmosphere beneath which weak  
205 downdrafts due to water loading take place. In the dissipating stage, moisture in the pol-  
206 luted run is more heavily distributed over the mid-to-low free atmosphere (Fig. 3d). The  
207 water vapor mixing ratio there is  $1.5 \text{ g kg}^{-1}$  more than that in the pristine run. The dif-  
208 ference may be caused by the stronger evaporation of raindrops as we found there is more  
209 mass but nearly the same number of falling raindrops beneath clouds in the polluted run  
210 leading to two times stronger surface precipitation (figure not shown). These raindrops  
211 could be from the melting of graupel and hail since the warm-rain process is suppressed  
212 due to pollution.

213 Past studies have shown that humidity in the lower free atmosphere is critical to  
214 the onset of tropical deep convection (Derbyshire et al., 2004; Holloway & Neelin, 2009,  
215 2010; Schiro et al., 2016; Tompkins, 2001). The enhanced moisture in the lower free at-  
216 mosphere increases the buoyancy of entraining plumes, leading to an increased chance  
217 of deep convection. The signal of the exceeding moisture in the mid-to-low free atmo-  
218 sphere in the polluted run extends to the CWV regimes of developing and mature con-  
219 vection (Fig. 3d), in which the increase in moisture in the mid-to-high atmosphere re-  
220 flects the prevalence of convection (Fig. 3a-b). The modulated moisture distribution, orig-  
221 inating from the response of dissipating stage of convection to changes in cloud micro-  
222 physics, enhances conditional instability, potentially contributing to the development of  
223 subsequent convection. Further investigations on the mechanism will be carried out in  
224 the future.

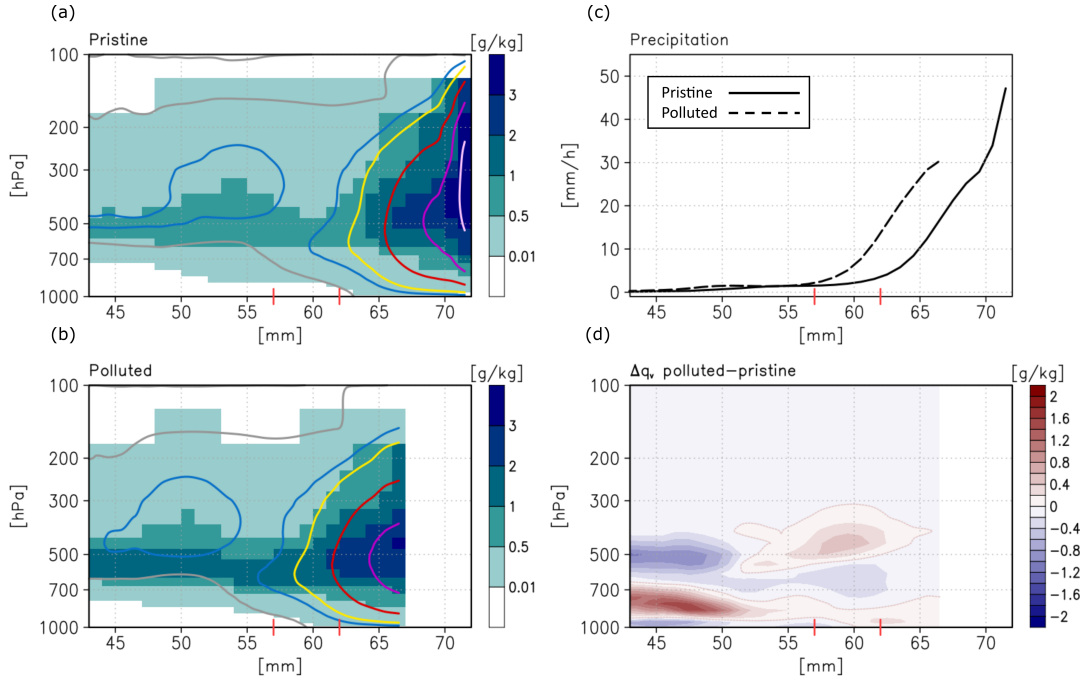


**Figure 3.** Mass mixing ratio of cloud water and cloud ice (shaded) and vertical velocity (contours at 0, 0.1, 0.2, 0.5, 1, 2  $\text{m s}^{-1}$ ) within the updraft regions of convective systems conditional sampled by column water vapor of the pristine (a) and the polluted (b) run from days 90 to 120. Precipitation intensity of the two runs (c) and the difference of water vapor mixing ratio (polluted run minus the pristine run) (d) sampled by the same method. The red dotted line in (d) shows the contour of 0  $\text{g kg}^{-1}$ . The red sticks along the x-axis show the CWV value of 57 and 62 mm

225 However, the highest CWV environment over the updraft regions ( $>67$  mm) in the  
 226 pristine run is absent in the polluted run (Fig. 3). The polluted run has notably drier  
 227 moist clusters (Fig. 2), leading to the weaker maximum intensity of updraft and precipi-  
 228 tation (30 vs. 47  $\text{mm h}^{-1}$ ). As the moisture distribution is maintained by large-scale cir-  
 229 culation, we investigate the influence of pollution on large-scale circulation by sorting  
 230 the distance to the nearest convective system and projecting horizontal winds in the di-  
 231 rection pointing to the nearest system (green contours in Fig. 1a). Large-scale circula-  
 232 tion has often been visualized with a streamfunction in moisture space when analyzing  
 233 self-aggregated runs to RCE (Arnold & Putman, 2018; Bretherton et al., 2005; Holloway  
 234 & Woolnough, 2016; C. Muller & Bony, 2015; C. J. Muller & Held, 2012). The stream-  
 235 function analyzed in past studies is designed to investigate the energy transport between  
 236 dry areas and moist clusters but it does not represent circulation in physical space. It  
 237 is natural to analyze large-scale circulation in physical space when using a global convec-  
 238 tion-permitting model with an appropriate choice of the source of momentum and energy trans-  
 239 port. The result shows that both runs exhibit typical structures of tropical circulation,  
 240 including low-level inflow, mid-level outflow, and deep convection outflow (Johnson et  
 241 al., 1999), but every component of the circulation is weaker in the polluted run (Fig. 4).

242 We trace the cause of the weaker large-scale circulation down to the influence of  
 243 pollution on the geographical distribution of convective systems (i.e., updraft regions).  
 244 In the polluted run, convective systems develop geographically closer to the meander-  
 245 ing margin (i.e., 43 mm) of moist clusters, because CWV increases monotonically from  
 246 dry areas toward moist clusters (Fig. 1b), and convection strength enhances more rapidly

247 as CWV increases in the polluted run (Fig. 3b). Fig. 2 shows that the average distance  
 248 from the edges of moist clusters to the nearest convective system in the pristine run is  
 249 1.5 times longer than that in the polluted run. Meanwhile, inhibiting the warm-rain pro-  
 250 cess by pollution could increase the mid-level static stability as a result of a latent heat-  
 251 ing dipole associated with the freezing water and melting ice above and below the freez-  
 252 ing level. Previous studies suggested that an increase in mid-level static stability pro-  
 253 motes detrainment (Johnson et al., 1999; Patrizio & Randall, 2019; Posselt et al., 2008,  
 254 2012). Overall, cloud condensates in the polluted run are more likely to be exported from  
 255 moist clusters to dry areas rather than stay in moist clusters and then re-evaporate. The  
 256 export of clouds impedes the moisture-convective feedback in which moistening environ-  
 257 ment by convection plays a key role in favoring subsequent development of convection  
 258 (W. Grabowski & Moncrieff, 2004; Holloway & Neelin, 2009). The above inference is sup-  
 259 ported by Fig. 4b, which shows that the exceeding cloud condensates in the polluted run  
 260 coincide with the mid-level outflow of the large-scale circulation.

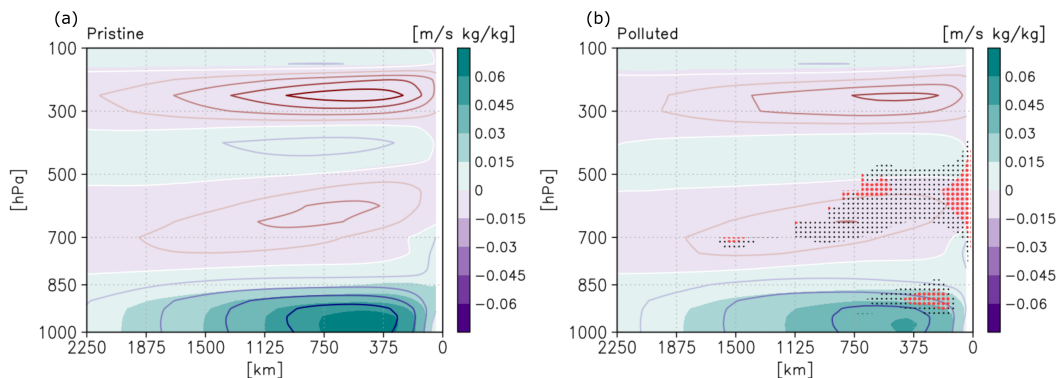


**Figure 4.** Water vapor flux (shaded) and horizontal winds (contours from  $-4$  to  $4$   $\text{m s}^{-1}$  with an interval of  $1$   $\text{m s}^{-1}$  using a color scale from maroon to white to navy) projected to the direction of pointing to the nearest convective system in the pristine (a) and the polluted (b) run from days 90 to 120. Positive values are vectors toward the system. The black and red dots in (b) show where the ratio of cloud water mixing ratio in the polluted run over the pristine one larger than 1 and 2, respectively

## 261 4 Summary and Discussion

262 This study investigates the response of tropical convection-circulation interaction  
 263 to enhanced CCN concentrations using non-rotating RCE simulations of a global convection-  
 264 permitting model run at  $15$  km horizontal resolution. Deep convection in the model is  
 265 represented in a way that the explicit simulation of convection seeds cloud-aerosol in-  
 266 teraction and is responsible for strong precipitation events. The simulations allow for the  
 267 large-scale organization of convection realistically inducing circulation without artificial  
 268 constraints of scale separation assumption, domain size, or domain shape. The novel find-  
 269 ing in this study is that pollution facilitates the development of deep convection in a drier  
 270 environment, while the response of large-scale circulation limits the intensity of maxi-  
 271 mum precipitation. Our results emphasize the importance of allowing atmospheric phe-  
 272 nomena to evolve continuously across spatial and temporal scales in simulations when  
 273 investigating the response of tropical convection to changes in cloud microphysics.

274 Connecting our result to the existing driving and maintaining mechanisms of CSA  
 275 could inspire future investigation on the response of global warming to varied CCN con-

276 concentrations since CSA is known to modulate climate sensitivity (Cronin & Wing, 2017).  
 277 The possible connections include:

- 278 1. The export of mid-level cloud condensates could weaken the radiatively driven sub-  
 279 sidence over the dry areas that drives CSA (Beydoun & Hoose, 2019; Bretherton  
 280 et al., 2005; C. J. Muller & Held, 2012; Wing & Emanuel, 2014; Holloway & Wool-  
 281 nough, 2016).
- 282 2. The response of cold pool dynamics to cloud microphysics has received consider-  
 283 able attention in the literature (Z. J. Lebo & Morrison, 2014; Seigel et al., 2013;  
 284 Storer et al., 2014; Su et al., 2020; Tao et al., 2007; van den Heever & Cotton, 2007).  
 285 Cold pools associated with the closer-to-edge convective systems in the polluted  
 286 run could mix low-level dry areas and moist clusters more effectively, weakening  
 287 the CSA (Jeevanjee & Romps, 2013; C. Muller & Bony, 2015).

288 Past studies (Arnold & Randall, 2015; Khairoutdinov & Emanuel, 2018) indicated  
 289 that the large-scale organization of convection (i.e., CSA) in non-rotating RCE simula-  
 290 tions and MJO-like (i.e., Madden-Julian Oscillation; Madden & Julian, 1971) disturbance  
 291 in rotating RCE simulations share the same driving mechanism (i.e., cloud-radiation feed-  
 292 backs) in which AIEs can be critical. One of the characteristics of MJO propagation is  
 293 that MJOs suffer from a barrier effect when it propagates over the Maritime Continent  
 294 (MC) (Kim et al., 2014; Zhang & Ling, 2017). The development of convective systems  
 295 over the water in the MC region plays a crucial role in carrying the MJO signal through  
 296 the MC (Ling et al., 2019). Around the globe, MC is a major source of different types  
 297 of aerosol (Reid et al., 2012; Salinas et al., 2013; Shpund et al., 2019). The modulation  
 298 of the size of moist clusters and the geographical distribution of convective systems by  
 299 enhanced CCN concentrations potentially provides a new perspective on the existing MJO  
 300 theories (Jiang et al., 2020; Zhang, 2013). A possible approach for the investigation is  
 301 to evaluate sub-seasonal hindcasts of an active MJO event with different aerosol emis-  
 302 sion scenarios.

## 303 5 Open Research

304 The model output data of a temporal snapshot, the Fortran program that computes  
 305 vertical atmospheric profiles conditional sampled by column water vapor and the distance  
 306 to the nearest convective system, and the GrADS plotting scripts in this study are avail-  
 307 able at <https://doi.org/10.6084/m9.figshare.22149617.v1>.

## 308 Acknowledgments

309 Chien-Ming Wu and Chun-Yian Su's efforts were supported by National Science and Tech-  
 310 nology Council (NSTC) in Taiwan grant 111-2111-M-002-012-NSTC. Wei-Ting Chen was  
 311 supported by Ministry of Science and Technology (MOST) in Taiwan grant 109-2628-  
 312 M-002-003-MY3. J. Peters was supported by National Science Foundation (NSF) grants  
 313 AGS-1928666, AGS-1841674, and the Department of Energy Atmospheric System Re-  
 314 search (DOE ASR) grant DE-SC0000246356. We thank Dr. Jen-Her Chen in Central  
 315 Weather Bureau for his support of this work.

## 316 References

- 317 Abbott, T. H., & Cronin, T. W. (2021, January). Aerosol invigoration of atmo-  
 318 spheric convection through increases in humidity. *Science*, *371*(6524), 83–85.  
 319 Retrieved from <https://doi.org/10.1126/science.abc5181> doi: 10.1126/  
 320 science.abc5181
- 321 Anber, U. M., Wang, S., Gentine, P., & Jensen, M. P. (2019, September). Prob-  
 322 ing the response of tropical deep convection to aerosol perturbations using

- 323 idealized cloud-resolving simulations with parameterized large-scale dynam-  
 324 ics. *Journal of the Atmospheric Sciences*, 76(9), 2885–2897. Retrieved from  
 325 <https://doi.org/10.1175/jas-d-18-0351.1> doi: 10.1175/jas-d-18-0351.1
- 326 Andreae, M. O. (2009, January). Correlation between cloud condensation nuclei  
 327 concentration and aerosol optical thickness in remote and polluted regions. *At-*  
 328 *mospheric Chemistry and Physics*, 9(2), 543–556. Retrieved from [https://doi](https://doi.org/10.5194/acp-9-543-2009)  
 329 [.org/10.5194/acp-9-543-2009](https://doi.org/10.5194/acp-9-543-2009) doi: 10.5194/acp-9-543-2009
- 330 Andreae, M. O., Rosenfeld, D., Artaxo, P., Costa, A. A., Frank, G. P., Longo,  
 331 K. M., & Silva-Dias, M. A. F. (2004, February). Smoking rain clouds over the  
 332 amazon. *Science*, 303(5662), 1337–1342. Retrieved from [https://doi.org/](https://doi.org/10.1126/science.1092779)  
 333 [10.1126/science.1092779](https://doi.org/10.1126/science.1092779) doi: 10.1126/science.1092779
- 334 Arakawa, A. (2004, July). The cumulus parameterization problem: Past, present,  
 335 and future. *Journal of Climate*, 17(13), 2493–2525. Retrieved from  
 336 [https://doi.org/10.1175/1520-0442\(2004\)017<2493:ratcpp>2.0.co;2](https://doi.org/10.1175/1520-0442(2004)017<2493:ratcpp>2.0.co;2)  
 337 doi: 10.1175/1520-0442(2004)017(2493:ratcpp)2.0.co;2
- 338 Arakawa, A., & Wu, C.-M. (2013, July). A unified representation of deep moist  
 339 convection in numerical modeling of the atmosphere. part i. *Journal of the At-*  
 340 *mospheric Sciences*, 70(7), 1977–1992. Retrieved from [https://doi.org/10](https://doi.org/10.1175/jas-d-12-0330.1)  
 341 [.1175/jas-d-12-0330.1](https://doi.org/10.1175/jas-d-12-0330.1) doi: 10.1175/jas-d-12-0330.1
- 342 Arnold, N. P., & Putman, W. M. (2018, April). Nonrotating convective self-  
 343 aggregation in a limited area AGCM. *Journal of Advances in Modeling Earth*  
 344 *Systems*, 10(4), 1029–1046. Retrieved from [https://doi.org/10.1002/](https://doi.org/10.1002/2017ms001218)  
 345 [2017ms001218](https://doi.org/10.1002/2017ms001218) doi: 10.1002/2017ms001218
- 346 Arnold, N. P., & Randall, D. A. (2015, October). Global-scale convective aggre-  
 347 gation: Implications for the madden-julian oscillation. *Journal of Advances in*  
 348 *Modeling Earth Systems*, 7(4), 1499–1518. Retrieved from [https://doi.org/](https://doi.org/10.1002/2015ms000498)  
 349 [10.1002/2015ms000498](https://doi.org/10.1002/2015ms000498) doi: 10.1002/2015ms000498
- 350 Beydoun, H., & Hoose, C. (2019, April). Aerosol-cloud-precipitation interactions  
 351 in the context of convective self-aggregation. *Journal of Advances in Modeling*  
 352 *Earth Systems*, 11(4), 1066–1087. Retrieved from [https://doi.org/10.1029/](https://doi.org/10.1029/2018ms001523)  
 353 [2018ms001523](https://doi.org/10.1029/2018ms001523) doi: 10.1029/2018ms001523
- 354 Bretherton, C. S., Blossey, P. N., & Khairoutdinov, M. (2005, December). An  
 355 energy-balance analysis of deep convective self-aggregation above uniform SST.  
 356 *Journal of the Atmospheric Sciences*, 62(12), 4273–4292. Retrieved from  
 357 <https://doi.org/10.1175/jas3614.1> doi: 10.1175/jas3614.1
- 358 Bretherton, C. S., Peters, M. E., & Back, L. E. (2004, April). Relationships be-  
 359 tween water vapor path and precipitation over the tropical oceans. *Jour-*  
 360 *nal of Climate*, 17(7), 1517–1528. Retrieved from [https://doi.org/](https://doi.org/10.1175/1520-0442(2004)017<1517:rbwvpa>2.0.co;2)  
 361 [10.1175/1520-0442\(2004\)017<1517:rbwvpa>2.0.co;2](https://doi.org/10.1175/1520-0442(2004)017<1517:rbwvpa>2.0.co;2)  
 362 doi: 10.1175/1520-0442(2004)017(1517:rbwvpa)2.0.co;2
- 363 Chang, Y.-H., Chen, W.-T., Wu, C.-M., Moseley, C., & Wu, C.-C. (2021, Novem-  
 364 ber). Tracking the influence of cloud condensation nuclei on summer diurnal  
 365 precipitating systems over complex topography in taiwan. *Atmospheric Chem-*  
 366 *istry and Physics*, 21(22), 16709–16725. Retrieved from [https://doi.org/](https://doi.org/10.5194/acp-21-16709-2021)  
 367 [10.5194/acp-21-16709-2021](https://doi.org/10.5194/acp-21-16709-2021) doi: 10.5194/acp-21-16709-2021
- 368 Chen, P.-J., Chen, W.-T., Wu, C.-M., & Yo, T.-S. (2021, May). Convective cloud  
 369 regimes from a classification of object-based CloudSat observations over asian-  
 370 australian monsoon areas. *Geophysical Research Letters*, 48(10). Retrieved  
 371 from <https://doi.org/10.1029/2021gl1092733> doi: 10.1029/2021gl1092733
- 372 Coppin, D., & Bony, S. (2015, December). Physical mechanisms controlling the  
 373 initiation of convective self-aggregation in a general circulation model. *Jour-*  
 374 *nal of Advances in Modeling Earth Systems*, 7(4), 2060–2078. Retrieved from  
 375 <https://doi.org/10.1002/2015ms000571> doi: 10.1002/2015ms000571
- 376 Cronin, T. W., & Wing, A. A. (2017, December). Clouds, circulation, and climate  
 377 sensitivity in a radiative-convective equilibrium channel model. *Journal of Ad-*

- 378 *vances in Modeling Earth Systems*, 9(8), 2883–2905. Retrieved from <https://doi.org/10.1002/2017ms001111> doi: 10.1002/2017ms001111
- 379
- 380 Derbyshire, S., Beau, I., Bechtold, P., Grandpeix, J.-Y., Piriou, J.-M., Redelsperger,  
381 J.-L., & Soares, P. (2004, October). Sensitivity of moist convection to envi-  
382 ronmental humidity. *Quarterly Journal of the Royal Meteorological Society*,  
383 130(604), 3055–3079. Retrieved from <https://doi.org/10.1256/qj.03.130>  
384 doi: 10.1256/qj.03.130
- 385 Dunion, J. P. (2011, February). Rewriting the climatology of the tropical north  
386 atlantic and caribbean sea atmosphere. *Journal of Climate*, 24(3), 893–  
387 908. Retrieved from <https://doi.org/10.1175/2010jcli3496.1> doi:  
388 10.1175/2010jcli3496.1
- 389 Emanuel, K., Wing, A. A., & Vincent, E. M. (2014, February). Radiative-  
390 convective instability. *Journal of Advances in Modeling Earth Systems*, 6(1),  
391 75–90. Retrieved from <https://doi.org/10.1002/2013ms000270> doi:  
392 10.1002/2013ms000270
- 393 Fan, J., & Khain, A. (2021, January). Comments on “do ultrafine cloud condensa-  
394 tion nuclei invigorate deep convection?”. *Journal of the Atmospheric Sciences*,  
395 78(1), 329–339. Retrieved from <https://doi.org/10.1175/jas-d-20-0218.1>  
396 doi: 10.1175/jas-d-20-0218.1
- 397 Fan, J., Rosenfeld, D., Zhang, Y., Giangrande, S. E., Li, Z., Machado, L. A. T.,  
398 ... de Souza, R. A. F. (2018, January). Substantial convection and pre-  
399 cipitation enhancements by ultrafine aerosol particles. *Science*, 359(6374),  
400 411–418. Retrieved from <https://doi.org/10.1126/science.aan8461> doi:  
401 10.1126/science.aan8461
- 402 Fan, J., Wang, Y., Rosenfeld, D., & Liu, X. (2016, October). Review of  
403 aerosol–cloud interactions: Mechanisms, significance, and challenges. *Jour-  
404 nal of the Atmospheric Sciences*, 73(11), 4221–4252. Retrieved from  
405 <https://doi.org/10.1175/jas-d-16-0037.1> doi: 10.1175/jas-d-16-0037.1
- 406 Fan, J., Yuan, T., Comstock, J. M., Ghan, S., Khain, A., Leung, L. R., ... Ovchin-  
407 nikov, M. (2009, November). Dominant role by vertical wind shear in regulat-  
408 ing aerosol effects on deep convective clouds. *Journal of Geophysical Research*,  
409 114(D22). Retrieved from <https://doi.org/10.1029/2009jd012352> doi:  
410 10.1029/2009jd012352
- 411 Forster, P., Storelvmo, T., Armour, K., Collins, W., Dufresne, J.-L., Frame, D., ...  
412 Zhang, H. (2021). The earth’s energy budget, climate feedbacks, and cli-  
413 mate sensitivity [Book Section]. In V. Masson-Delmotte et al. (Eds.), *Climate  
414 change 2021: The physical science basis. contribution of working group i to  
415 the sixth assessment report of the intergovernmental panel on climate change*  
416 (p. 923–1054). Cambridge, United Kingdom and New York, NY, USA: Cam-  
417 bridge University Press. doi: 10.1017/9781009157896.009
- 418 Grabowski, W., & Moncrieff, M. (2004, October). Moisture–convection feedback in  
419 the tropics. *Quarterly Journal of the Royal Meteorological Society*, 130(604),  
420 3081–3104. Retrieved from <https://doi.org/10.1256/qj.03.135> doi: 10.  
421 1256/qj.03.135
- 422 Grabowski, W. W. (2018, October). Can the impact of aerosols on deep convec-  
423 tion be isolated from meteorological effects in atmospheric observations? *Jour-  
424 nal of the Atmospheric Sciences*, 75(10), 3347–3363. Retrieved from <https://doi.org/10.1175/jas-d-18-0105.1> doi: 10.1175/jas-d-18-0105.1
- 425
- 426 Grabowski, W. W., & Morrison, H. (2020, July). Do ultrafine cloud condensation  
427 nuclei invigorate deep convection? *Journal of the Atmospheric Sciences*, 77(7),  
428 2567–2583. Retrieved from <https://doi.org/10.1175/jas-d-20-0012.1> doi:  
429 10.1175/jas-d-20-0012.1
- 430 Grabowski, W. W., & Morrison, H. (2021, January). Reply to “comments on ‘do ul-  
431 tra-fine cloud condensation nuclei invigorate deep convection?’”. *Journal of the  
432 Atmospheric Sciences*, 78(1), 341–350. Retrieved from <https://doi.org/10>

- 433 .1175/jas-d-20-0315.1 doi: 10.1175/jas-d-20-0315.1
- 434 Hamada, A., Murayama, Y., & Takayabu, Y. N. (2014, October). Regional charac-  
 435 teristics of extreme rainfall extracted from TRMM PR measurements. *Journal*  
 436 *of Climate*, 27(21), 8151–8169. Retrieved from [https://doi.org/10.1175/](https://doi.org/10.1175/jcli-d-14-00107.1)  
 437 [jcli-d-14-00107.1](https://doi.org/10.1175/jcli-d-14-00107.1) doi: 10.1175/jcli-d-14-00107.1
- 438 Hartmann, D. L., Moy, L. A., & Fu, Q. (2001, December). Tropical convection and  
 439 the energy balance at the top of the atmosphere. *Journal of Climate*, 14(24),  
 440 4495–4511. Retrieved from [https://doi.org/10.1175/1520-0442\(2001\)](https://doi.org/10.1175/1520-0442(2001)014<4495:tcateb>2.0.co;2)  
 441 [014<4495:tcateb>2.0.co;2](https://doi.org/10.1175/1520-0442(2001)014<4495:tcateb>2.0.co;2) doi: 10.1175/1520-0442(2001)014<4495:  
 442 [tcateb>2.0.co;2](https://doi.org/10.1175/1520-0442(2001)014<4495:tcateb>2.0.co;2)
- 443 Holloway, C. E., & Neelin, J. D. (2009, June). Moisture vertical structure, col-  
 444 umn water vapor, and tropical deep convection. *Journal of the Atmospheric*  
 445 *Sciences*, 66(6), 1665–1683. Retrieved from [https://doi.org/10.1175/](https://doi.org/10.1175/2008jas2806.1)  
 446 [2008jas2806.1](https://doi.org/10.1175/2008jas2806.1) doi: 10.1175/2008jas2806.1
- 447 Holloway, C. E., & Neelin, J. D. (2010, April). Temporal relations of column water  
 448 vapor and tropical precipitation. *Journal of the Atmospheric Sciences*, 67(4),  
 449 1091–1105. Retrieved from <https://doi.org/10.1175/2009jas3284.1> doi:  
 450 [10.1175/2009jas3284.1](https://doi.org/10.1175/2009jas3284.1)
- 451 Holloway, C. E., & Woolnough, S. J. (2016, February). The sensitivity of convective  
 452 aggregation to diabatic processes in idealized radiative-convective equilib-  
 453 rium simulations. *Journal of Advances in Modeling Earth Systems*, 8(1),  
 454 166–195. Retrieved from <https://doi.org/10.1002/2015ms000511> doi:  
 455 [10.1002/2015ms000511](https://doi.org/10.1002/2015ms000511)
- 456 Houze, R. A. (2004, December). Mesoscale convective systems. *Reviews of Geo-*  
 457 *physics*, 42(4). Retrieved from <https://doi.org/10.1029/2004rg000150>  
 458 doi: 10.1029/2004rg000150
- 459 Houze, R. A., Rasmussen, K. L., Zuluaga, M. D., & Brodzik, S. R. (2015, Septem-  
 460 ber). The variable nature of convection in the tropics and subtropics: A legacy  
 461 of 16 years of the tropical rainfall measuring mission satellite. *Reviews of*  
 462 *Geophysics*, 53(3), 994–1021. Retrieved from [https://doi.org/10.1002/](https://doi.org/10.1002/2015rg000488)  
 463 [2015rg000488](https://doi.org/10.1002/2015rg000488) doi: 10.1002/2015rg000488
- 464 Igel, A. L., & van den Heever, S. C. (2021, August). Invigoration or enervation of  
 465 convective clouds by aerosols? *Geophysical Research Letters*, 48(16). Retrieved  
 466 from <https://doi.org/10.1029/2021gl093804> doi: 10.1029/2021gl093804
- 467 Jeevanjee, N., & Romps, D. M. (2013, March). Convective self-aggregation, cold  
 468 pools, and domain size. *Geophysical Research Letters*, 40(5), 994–998. Re-  
 469 trieved from <https://doi.org/10.1002/grl.50204> doi: 10.1002/grl.50204
- 470 Jiang, X., Adames, Á. F., Kim, D., Maloney, E. D., Lin, H., Kim, H., . . . Klinga-  
 471 man, N. P. (2020, August). Fifty years of research on the madden-julian  
 472 oscillation: Recent progress, challenges, and perspectives. *Journal of Geo-*  
 473 *physical Research: Atmospheres*, 125(17). Retrieved from [https://doi.org/](https://doi.org/10.1029/2019jd030911)  
 474 [10.1029/2019jd030911](https://doi.org/10.1029/2019jd030911) doi: 10.1029/2019jd030911
- 475 Johnson, R. H., Rickenbach, T. M., Rutledge, S. A., Ciesielski, P. E., & Schu-  
 476 bert, W. H. (1999, August). Trimodal characteristics of tropical convec-  
 477 tion. *Journal of Climate*, 12(8), 2397–2418. Retrieved from [https://](https://doi.org/10.1175/1520-0442(1999)012<2397:tcotc>2.0.co;2)  
 478 [doi.org/10.1175/1520-0442\(1999\)012<2397:tcotc>2.0.co;2](https://doi.org/10.1175/1520-0442(1999)012<2397:tcotc>2.0.co;2) doi:  
 479 [10.1175/1520-0442\(1999\)012<2397:tcotc>2.0.co;2](https://doi.org/10.1175/1520-0442(1999)012<2397:tcotc>2.0.co;2)
- 480 Khain, A. P., BenMoshe, N., & Pokrovsky, A. (2008, June). Factors determining the  
 481 impact of aerosols on surface precipitation from clouds: An attempt at classifi-  
 482 cation. *Journal of the Atmospheric Sciences*, 65(6), 1721–1748. Retrieved from  
 483 <https://doi.org/10.1175/2007jas2515.1> doi: 10.1175/2007jas2515.1
- 484 Khairoutdinov, M. F., & Emanuel, K. (2018, December). Intraseasonal variability in  
 485 a cloud-permitting near-global equatorial aquaplanet model. *Journal of the At-*  
 486 *mospheric Sciences*, 75(12), 4337–4355. Retrieved from [https://doi.org/10](https://doi.org/10.1175/jas-d-18-0152.1)  
 487 [.1175/jas-d-18-0152.1](https://doi.org/10.1175/jas-d-18-0152.1) doi: 10.1175/jas-d-18-0152.1

- 488 Kim, D., Kug, J.-S., & Sobel, A. H. (2014, January). Propagating versus non-  
 489 propagating madden–julian oscillation events. *Journal of Climate*, *27*(1),  
 490 111–125. Retrieved from <https://doi.org/10.1175/jcli-d-13-00084.1>  
 491 doi: 10.1175/jcli-d-13-00084.1
- 492 Koren, I., Feingold, G., & Remer, L. A. (2010, September). The invigoration  
 493 of deep convective clouds over the atlantic: aerosol effect, meteorology or  
 494 retrieval artifact? *Atmospheric Chemistry and Physics*, *10*(18), 8855–  
 495 8872. Retrieved from <https://doi.org/10.5194/acp-10-8855-2010> doi:  
 496 10.5194/acp-10-8855-2010
- 497 Koren, I., Martins, J. V., Remer, L. A., & Afargan, H. (2008, August). Smoke invig-  
 498 oration versus inhibition of clouds over the amazon. *Science*, *321*(5891), 946–  
 499 949. Retrieved from <https://doi.org/10.1126/science.1159185> doi: 10  
 500 .1126/science.1159185
- 501 Lebo, Z. (2018, February). A numerical investigation of the potential effects of  
 502 aerosol-induced warming and updraft width and slope on updraft intensity  
 503 in deep convective clouds. *Journal of the Atmospheric Sciences*, *75*(2), 535–  
 504 554. Retrieved from <https://doi.org/10.1175/jas-d-16-0368.1> doi:  
 505 10.1175/jas-d-16-0368.1
- 506 Lebo, Z. J., & Morrison, H. (2014, March). Dynamical effects of aerosol perturba-  
 507 tions on simulated idealized squall lines. *Monthly Weather Review*, *142*(3),  
 508 991–1009. Retrieved from <https://doi.org/10.1175/mwr-d-13-00156.1>  
 509 doi: 10.1175/mwr-d-13-00156.1
- 510 Ling, J., Zhang, C., Joyce, R., ping Xie, P., & Chen, G. (2019, March). Possible role  
 511 of the diurnal cycle in land convection in the barrier effect on the MJO by the  
 512 maritime continent. *Geophysical Research Letters*, *46*(5), 3001–3011. Retrieved  
 513 from <https://doi.org/10.1029/2019gl081962> doi: 10.1029/2019gl081962
- 514 Madden, R. A., & Julian, P. R. (1971, July). Detection of a 40–50 day oscillation  
 515 in the zonal wind in the tropical pacific. *Journal of the Atmospheric Sciences*,  
 516 *28*(5), 702–708. Retrieved from [https://doi.org/10.1175/1520-0469\(1971\)  
 517 028<0702:doadoi>2.0.co;2](https://doi.org/10.1175/1520-0469(1971)028<0702:doadoi>2.0.co;2) doi: 10.1175/1520-0469(1971)028<0702:doadoi>2  
 518 .0.co;2
- 519 Manabe, S., & Strickler, R. F. (1964, July). Thermal equilibrium of the atmosphere  
 520 with a convective adjustment. *Journal of the Atmospheric Sciences*, *21*(4),  
 521 361–385. Retrieved from [https://doi.org/10.1175/1520-0469\(1964\)  
 522 021<0361:teotaw>2.0.co;2](https://doi.org/10.1175/1520-0469(1964)021<0361:teotaw>2.0.co;2) doi: 10.1175/1520-0469(1964)021<0361:  
 523 teotaw>2.0.co;2
- 524 Matsugishi, S., & Satoh, M. (2022, May). Sensitivity of the horizontal scale  
 525 of convective self-aggregation to sea surface temperature in radiative con-  
 526 vective equilibrium experiments using a global nonhydrostatic model.  
 527 *Journal of Advances in Modeling Earth Systems*, *14*(5). Retrieved from  
 528 <https://doi.org/10.1029/2021ms002636> doi: 10.1029/2021ms002636
- 529 Morrison, H., & Milbrandt, J. A. (2015, January). Parameterization of cloud micro-  
 530 physics based on the prediction of bulk ice particle properties. part i: Scheme  
 531 description and idealized tests. *Journal of the Atmospheric Sciences*, *72*(1),  
 532 287–311. Retrieved from <https://doi.org/10.1175/jas-d-14-0065.1> doi:  
 533 10.1175/jas-d-14-0065.1
- 534 Muller, C., & Bony, S. (2015, July). What favors convective aggregation and why?  
 535 *Geophysical Research Letters*, *42*(13), 5626–5634. Retrieved from [https://doi  
 536 .org/10.1002/2015gl064260](https://doi.org/10.1002/2015gl064260) doi: 10.1002/2015gl064260
- 537 Muller, C., Yang, D., Craig, G., Cronin, T., Fildier, B., Haerter, J. O., ... Sher-  
 538 wood, S. C. (2022, January). Spontaneous aggregation of convective  
 539 storms. *Annual Review of Fluid Mechanics*, *54*(1), 133–157. Retrieved  
 540 from <https://doi.org/10.1146/annurev-fluid-022421-011319> doi:  
 541 10.1146/annurev-fluid-022421-011319
- 542 Muller, C. J., & Held, I. M. (2012, August). Detailed investigation of the self-

- 543 aggregation of convection in cloud-resolving simulations. *Journal of the At-*  
 544 *mospheric Sciences*, 69(8), 2551–2565. Retrieved from [https://doi.org/](https://doi.org/10.1175/jas-d-11-0257.1)  
 545 [10.1175/jas-d-11-0257.1](https://doi.org/10.1175/jas-d-11-0257.1) doi: 10.1175/jas-d-11-0257.1
- 546 Neelin, J. D., Peters, O., & Hales, K. (2009, August). The transition to strong con-  
 547 vection. *Journal of the Atmospheric Sciences*, 66(8), 2367–2384. Retrieved  
 548 from <https://doi.org/10.1175/2009jas2962.1> doi: 10.1175/2009jas2962  
 549 .1
- 550 Nesbitt, S. W., Cifelli, R., & Rutledge, S. A. (2006, October). Storm morphology  
 551 and rainfall characteristics of TRMM precipitation features. *Monthly Weather*  
 552 *Review*, 134(10), 2702–2721. Retrieved from [https://doi.org/10.1175/](https://doi.org/10.1175/mwr3200.1)  
 553 [mwr3200.1](https://doi.org/10.1175/mwr3200.1) doi: 10.1175/mwr3200.1
- 554 Nishant, N., & Sherwood, S. C. (2017, June). A cloud-resolving model study of  
 555 aerosol-cloud correlation in a pristine maritime environment. *Geophysical*  
 556 *Research Letters*, 44(11), 5774–5781. Retrieved from [https://doi.org/](https://doi.org/10.1002/2017gl073267)  
 557 [10.1002/2017gl073267](https://doi.org/10.1002/2017gl073267) doi: 10.1002/2017gl073267
- 558 Niu, F., & Li, Z. (2012, September). Systematic variations of cloud top tempera-  
 559 ture and precipitation rate with aerosols over the global tropics. *Atmospheric*  
 560 *Chemistry and Physics*, 12(18), 8491–8498. Retrieved from [https://doi.org/](https://doi.org/10.5194/acp-12-8491-2012)  
 561 [10.5194/acp-12-8491-2012](https://doi.org/10.5194/acp-12-8491-2012) doi: 10.5194/acp-12-8491-2012
- 562 Pan, Z., Rosenfeld, D., Zhu, Y., Mao, F., Gong, W., Zang, L., & Lu, X. (2021,  
 563 May). Observational quantification of aerosol invigoration for deep convective  
 564 cloud lifecycle properties based on geostationary satellite. *Journal of Geo-*  
 565 *physical Research: Atmospheres*, 126(9). Retrieved from [https://doi.org/](https://doi.org/10.1029/2020jd034275)  
 566 [10.1029/2020jd034275](https://doi.org/10.1029/2020jd034275) doi: 10.1029/2020jd034275
- 567 Patrizio, C. R., & Randall, D. A. (2019, July). Sensitivity of convective self-  
 568 aggregation to domain size. *Journal of Advances in Modeling Earth Systems*,  
 569 11(7), 1995–2019. Retrieved from <https://doi.org/10.1029/2019ms001672>  
 570 doi: 10.1029/2019ms001672
- 571 Pendergrass, A. G., Reed, K. A., & Medeiros, B. (2016, November). The link be-  
 572 tween extreme precipitation and convective organization in a warming climate:  
 573 Global radiative-convective equilibrium simulations. *Geophysical Research Let-*  
 574 *ters*, 43(21). Retrieved from <https://doi.org/10.1002/2016gl071285> doi:  
 575 [10.1002/2016gl071285](https://doi.org/10.1002/2016gl071285)
- 576 Peters, O., & Neelin, J. D. (2006, May). Critical phenomena in atmospheric precip-  
 577 itation. *Nature Physics*, 2(6), 393–396. Retrieved from [https://doi.org/10](https://doi.org/10.1038/nphys314)  
 578 [.1038/nphys314](https://doi.org/10.1038/nphys314) doi: 10.1038/nphys314
- 579 Popke, D., Stevens, B., & Voigt, A. (2013, January). Climate and climate change  
 580 in a radiative-convective equilibrium version of ECHAM6. *Journal of Advances*  
 581 *in Modeling Earth Systems*, 5(1), 1–14. Retrieved from [https://doi.org/10](https://doi.org/10.1029/2012ms000191)  
 582 [.1029/2012ms000191](https://doi.org/10.1029/2012ms000191) doi: 10.1029/2012ms000191
- 583 Posselt, D. J., van den Heever, S., Stephens, G., & Igel, M. R. (2012, January).  
 584 Changes in the interaction between tropical convection, radiation, and the  
 585 large-scale circulation in a warming environment. *Journal of Climate*, 25(2),  
 586 557–571. Retrieved from <https://doi.org/10.1175/2011jcli4167.1> doi:  
 587 [10.1175/2011jcli4167.1](https://doi.org/10.1175/2011jcli4167.1)
- 588 Posselt, D. J., van den Heever, S. C., & Stephens, G. L. (2008, April). Tri-  
 589 modal cloudiness and tropical stable layers in simulations of radiative con-  
 590 vective equilibrium. *Geophysical Research Letters*, 35(8). Retrieved from  
 591 <https://doi.org/10.1029/2007gl033029> doi: 10.1029/2007gl033029
- 592 Reid, J. S., Xian, P., Hyer, E. J., Flatau, M. K., Ramirez, E. M., Turk, F. J., ...  
 593 Maloney, E. D. (2012, February). Multi-scale meteorological conceptual  
 594 analysis of observed active fire hotspot activity and smoke optical depth in  
 595 the maritime continent. *Atmospheric Chemistry and Physics*, 12(4), 2117–  
 596 2147. Retrieved from <https://doi.org/10.5194/acp-12-2117-2012> doi:  
 597 [10.5194/acp-12-2117-2012](https://doi.org/10.5194/acp-12-2117-2012)

- 598 Rosenfeld, D., Lohmann, U., Raga, G. B., O'Dowd, C. D., Kulmala, M., Fuzzi,  
599 S., ... Andreae, M. O. (2008, September). Flood or drought: How do  
600 aerosols affect precipitation? *Science*, *321*(5894), 1309–1313. Retrieved from  
601 <https://doi.org/10.1126/science.1160606> doi: 10.1126/science.1160606
- 602 Salinas, S. V., Chew, B. N., Miettinen, J., Campbell, J. R., Welton, E. J., Reid,  
603 J. S., ... Liew, S. C. (2013, March). Physical and optical characteristics of  
604 the october 2010 haze event over singapore: A photometric and lidar analy-  
605 sis. *Atmospheric Research*, *122*, 555–570. Retrieved from [https://doi.org/](https://doi.org/10.1016/j.atmosres.2012.05.021)  
606 [10.1016/j.atmosres.2012.05.021](https://doi.org/10.1016/j.atmosres.2012.05.021) doi: 10.1016/j.atmosres.2012.05.021
- 607 Schiro, K. A., Neelin, J. D., Adams, D. K., & Lintner, B. R. (2016, September).  
608 Deep convection and column water vapor over tropical land versus tropical  
609 ocean: A comparison between the amazon and the tropical western pacific.  
610 *Journal of the Atmospheric Sciences*, *73*(10), 4043–4063. Retrieved from  
611 <https://doi.org/10.1175/jas-d-16-0119.1> doi: 10.1175/jas-d-16-0119.1
- 612 Seigel, R. B., van den Heever, S. C., & Saleeby, S. M. (2013, April). Mineral  
613 dust indirect effects and cloud radiative feedbacks of a simulated idealized  
614 nocturnal squall line. *Atmospheric Chemistry and Physics*, *13*(8), 4467–  
615 4485. Retrieved from <https://doi.org/10.5194/acp-13-4467-2013> doi:  
616 10.5194/acp-13-4467-2013
- 617 Shpund, J., Khain, A., & Rosenfeld, D. (2019, August). Effects of sea spray on mi-  
618 crophysics and intensity of deep convective clouds under strong winds. *Jour-  
619 nal of Geophysical Research: Atmospheres*, *124*(16), 9484–9509. Retrieved from  
620 <https://doi.org/10.1029/2018jd029893> doi: 10.1029/2018jd029893
- 621 Singh, M. S., & O'Gorman, P. A. (2013, August). Influence of entrainment  
622 on the thermal stratification in simulations of radiative-convective equilib-  
623 rium. *Geophysical Research Letters*, *40*(16), 4398–4403. Retrieved from  
624 <https://doi.org/10.1002/grl.50796> doi: 10.1002/grl.50796
- 625 Singh, M. S., & O'Gorman, P. A. (2015, June). Increases in moist-convective up-  
626 draught velocities with warming in radiative-convective equilibrium. *Quarterly  
627 Journal of the Royal Meteorological Society*, *141*(692), 2828–2838. Retrieved  
628 from <https://doi.org/10.1002/qj.2567> doi: 10.1002/qj.2567
- 629 Sobel, A. H., Nilsson, J., & Polvani, L. M. (2001, December). The weak temper-  
630 ature gradient approximation and balanced tropical moisture waves. *Journal  
631 of the Atmospheric Sciences*, *58*(23), 3650–3665. Retrieved from [https://doi  
632 .org/10.1175/1520-0469\(2001\)058<3650:twtgaa>2.0.co;2](https://doi.org/10.1175/1520-0469(2001)058<3650:twtgaa>2.0.co;2) doi: 10.1175/  
633 1520-0469(2001)058(3650:twtgaa)2.0.co;2
- 634 Stevens, B., Satoh, M., Auger, L., Biercamp, J., Bretherton, C. S., Chen, X., ...  
635 Zhou, L. (2019, September). DYAMOND: the DYnamics of the atmospheric  
636 general circulation modeled on non-hydrostatic domains. *Progress in Earth  
637 and Planetary Science*, *6*(1). Retrieved from [https://doi.org/10.1186/  
638 s40645-019-0304-z](https://doi.org/10.1186/s40645-019-0304-z) doi: 10.1186/s40645-019-0304-z
- 639 Storer, R. L., van den Heever, S. C., & L'Ecuyer, T. S. (2014, April). Observations  
640 of aerosol-induced convective invigoration in the tropical east atlantic. *Jour-  
641 nal of Geophysical Research: Atmospheres*, *119*(7), 3963–3975. Retrieved from  
642 <https://doi.org/10.1002/2013jd020272> doi: 10.1002/2013jd020272
- 643 Su, C.-Y., Chen, W.-T., Chen, J.-P., Chang, W.-Y., & Jou, B. J.-D. (2020). The  
644 impacts of cloud condensation nuclei on the extreme precipitation of a mon-  
645 soon coastal mesoscale convection system. *Terrestrial, Atmospheric and  
646 Oceanic Sciences*, *31*(2), 131–139. Retrieved from [https://doi.org/10.3319/  
647 tao.2019.11.29.01](https://doi.org/10.3319/tao.2019.11.29.01) doi: 10.3319/tao.2019.11.29.01
- 648 SU, C.-Y., CHEN, W.-T., WU, C.-M., & MA, H.-Y. (2022). Object-based eval-  
649 uation of tropical precipitation systems in DYAMOND simulations over the  
650 maritime continent. *Journal of the Meteorological Society of Japan. Ser. II*,  
651 *100*(4), 647–659. Retrieved from <https://doi.org/10.2151/jmsj.2022-033>  
652 doi: 10.2151/jmsj.2022-033

- 553 Su, C.-Y., Wu, C.-M., Chen, W.-T., & Chen, J.-H. (2021a, July). The effects of  
 554 the unified parameterization in the CWBGFS: the diurnal cycle of precip-  
 555 itation over land in the maritime continent. *Climate Dynamics*, *58*(1-2),  
 556 223–233. Retrieved from <https://doi.org/10.1007/s00382-021-05899-2>  
 557 doi: 10.1007/s00382-021-05899-2
- 558 Su, C.-Y., Wu, C.-M., Chen, W.-T., & Chen, J.-H. (2021b, October). Implementa-  
 559 tion of the unified representation of deep moist convection in the CWBGFS.  
 560 *Monthly Weather Review*, *149*(10), 3525–3539. Retrieved from [https://](https://doi.org/10.1175/mwr-d-21-0067.1)  
 561 [doi.org/10.1175/mwr-d-21-0067.1](https://doi.org/10.1175/mwr-d-21-0067.1) doi: 10.1175/mwr-d-21-0067.1
- 562 Tao, W.-K., Chen, J.-P., Li, Z., Wang, C., & Zhang, C. (2012, April). Impact  
 563 of aerosols on convective clouds and precipitation. *Reviews of Geophysics*,  
 564 *50*(2). Retrieved from <https://doi.org/10.1029/2011rg000369> doi:  
 565 10.1029/2011rg000369
- 566 Tao, W.-K., & Chern, J.-D. (2017, April). The impact of simulated mesoscale  
 567 convective systems on global precipitation: A multiscale modeling study. *Jour-  
 568 nal of Advances in Modeling Earth Systems*, *9*(2), 790–809. Retrieved from  
 569 <https://doi.org/10.1002/2016ms000836> doi: 10.1002/2016ms000836
- 570 Tao, W.-K., Li, X., Khain, A., Matsui, T., Lang, S., & Simpson, J. (2007, Decem-  
 571 ber). Role of atmospheric aerosol concentration on deep convective precipi-  
 572 tation: Cloud-resolving model simulations. *Journal of Geophysical Research*,  
 573 *112*(D24). Retrieved from <https://doi.org/10.1029/2007jd008728> doi:  
 574 10.1029/2007jd008728
- 575 Tompkins, A. M. (2001, March). Organization of tropical convection in low verti-  
 576 cal wind shears: The role of water vapor. *Journal of the Atmospheric Sciences*,  
 577 *58*(6), 529–545. Retrieved from [https://doi.org/10.1175/1520-0469\(2001\)](https://doi.org/10.1175/1520-0469(2001)058<0529:ootcil>2.0.co;2)  
 578 [058<0529:ootcil>2.0.co;2](https://doi.org/10.1175/1520-0469(2001)058(0529:ootcil)2.0.co;2) doi: 10.1175/1520-0469(2001)058(0529:ootcil)2.0  
 579 .co;2
- 580 Tsai, W.-M., & Wu, C.-M. (2017, September). The environment of aggregated  
 581 deep convection. *Journal of Advances in Modeling Earth Systems*, *9*(5), 2061–  
 582 2078. Retrieved from <https://doi.org/10.1002/2017ms000967> doi: 10  
 583 .1002/2017ms000967
- 584 van den Heever, S. C., & Cotton, W. R. (2007, June). Urban aerosol impacts on  
 585 downwind convective storms. *Journal of Applied Meteorology and Climatology*,  
 586 *46*(6), 828–850. Retrieved from <https://doi.org/10.1175/jam2492.1> doi:  
 587 10.1175/jam2492.1
- 588 van den Heever, S. C., Stephens, G. L., & Wood, N. B. (2011, April). Aerosol  
 589 indirect effects on tropical convection characteristics under conditions of ra-  
 590 diative–convective equilibrium. *Journal of the Atmospheric Sciences*, *68*(4),  
 591 699–718. Retrieved from <https://doi.org/10.1175/2010jas3603.1> doi:  
 592 10.1175/2010jas3603.1
- 593 Varble, A. (2018, April). Erroneous attribution of deep convective invigoration to  
 594 aerosol concentration. *Journal of the Atmospheric Sciences*, *75*(4), 1351–1368.  
 595 Retrieved from <https://doi.org/10.1175/jas-d-17-0217.1> doi: 10.1175/  
 596 jas-d-17-0217.1
- 597 Wing, A. A., Emanuel, K., Holloway, C. E., & Muller, C. (2017, February). Con-  
 598 vective self-aggregation in numerical simulations: A review. *Surveys in Geo-  
 599 physics*, *38*(6), 1173–1197. Retrieved from [https://doi.org/10.1007/s10712-](https://doi.org/10.1007/s10712-017-9408-4)  
 600 [017-9408-4](https://doi.org/10.1007/s10712-017-9408-4) doi: 10.1007/s10712-017-9408-4
- 601 Wing, A. A., & Emanuel, K. A. (2014, February). Physical mechanisms controlling  
 602 self-aggregation of convection in idealized numerical modeling simulations.  
 603 *Journal of Advances in Modeling Earth Systems*, *6*(1), 59–74. Retrieved from  
 604 <https://doi.org/10.1002/2013ms000269> doi: 10.1002/2013ms000269
- 605 Wing, A. A., Reed, K. A., Satoh, M., Stevens, B., Bony, S., & Ohno, T. (2018,  
 606 March). Radiative–convective equilibrium model intercomparison project.  
 607 *Geoscientific Model Development*, *11*(2), 793–813. Retrieved from <https://>

- 708 doi.org/10.5194/gmd-11-793-2018 doi: 10.5194/gmd-11-793-2018  
709 Wing, A. A., Stauffer, C. L., Becker, T., Reed, K. A., Ahn, M.-S., Arnold, N. P.,  
710 ... Zhao, M. (2020, September). Clouds and convective self-aggregation  
711 in a multimodel ensemble of radiative-convective equilibrium simulations.  
712 *Journal of Advances in Modeling Earth Systems*, 12(9). Retrieved from  
713 <https://doi.org/10.1029/2020ms002138> doi: 10.1029/2020ms002138  
714 Wu, C.-M., & Arakawa, A. (2014, May). A unified representation of deep moist con-  
715 vection in numerical modeling of the atmosphere. part II. *Journal of the At-*  
716 *mospheric Sciences*, 71(6), 2089–2103. Retrieved from [https://doi.org/10](https://doi.org/10.1175/jas-d-13-0382.1)  
717 [.1175/jas-d-13-0382.1](https://doi.org/10.1175/jas-d-13-0382.1) doi: 10.1175/jas-d-13-0382.1  
718 Yanase, T., Nishizawa, S., Miura, H., & Tomita, H. (2022, September). Character-  
719 istic form and distance in high-level hierarchical structure of self-aggregated  
720 clouds in radiative-convective equilibrium. *Geophysical Research Letters*,  
721 49(18). Retrieved from <https://doi.org/10.1029/2022gl1100000> doi:  
722 10.1029/2022gl1100000  
723 Yuan, J., & Houze, R. A. (2010, November). Global variability of mesoscale con-  
724 vective system anvil structure from a-train satellite data. *Journal of Climate*,  
725 23(21), 5864–5888. Retrieved from [https://doi.org/10.1175/2010jcli3671](https://doi.org/10.1175/2010jcli3671.1)  
726 [.1](https://doi.org/10.1175/2010jcli3671.1) doi: 10.1175/2010jcli3671.1  
727 Zhang, C. (2013, December). Madden–julian oscillation: Bridging weather and cli-  
728 mate. *Bulletin of the American Meteorological Society*, 94(12), 1849–1870. Re-  
729 trieved from <https://doi.org/10.1175/bams-d-12-00026.1> doi: 10.1175/  
730 [bams-d-12-00026.1](https://doi.org/10.1175/bams-d-12-00026.1)  
731 Zhang, C., & Ling, J. (2017, May). Barrier effect of the indo-pacific maritime con-  
732 tinent on the MJO: Perspectives from tracking MJO precipitation. *Journal of*  
733 *Climate*, 30(9), 3439–3459. Retrieved from [https://doi.org/10.1175/jcli](https://doi.org/10.1175/jcli-d-16-0614.1)  
734 [-d-16-0614.1](https://doi.org/10.1175/jcli-d-16-0614.1) doi: 10.1175/jcli-d-16-0614.1